OUTGASSING OF CHONDRITIC PLANETS

by

Dushan Stephen Bukvic

S.B. Massachusetts Institute of Technology
S.B. Massachusetts Institute of Technology
1976

SUBMITTED IN PARTIAL FULFILLMENT

OF THE REQUIREMENTS FOR THE

DEGREE OF MASTER OF

SCIENCE

at the

MASSACHUSETTS INSTITUTE OF

TECHNOLOGY

September, 1979

Signature of Author . . . . . .
Department of Earth and Planetary Sciences
September 18, 1979

Certified by . . . . . .
Thesis Supervisor

Accepted by . . . . . .
Chairman, Departmental Committee

OUTGASSING OF CHONDRITIC PLANETS

Dushan Stephen Bukvic

Submitted to the Department of Earth and Planetary Sciences on September 18, 1979 in partial fulfillment of the requirements for the degree of Master of Science.

Time-dependent chemical equilibrium outgassing histories of primitive, undifferentiated chondritic planets are presented. The compositions considered range from an ordinary chondrite model to a model of 90% ordinary chondrite + 10% Cl carbonaceous chondrite material. The sequence of mineralogical changes in the surface regions of these models due to oxidation by outgassing of volatiles is investigated up to the disappearance of metallic iron. The time-dependent equilibrium chemistry of many compounds and gases and the evolution of a 'raw' atmosphere are presented. Applications of these models to the Solar System are proposed.

Thesis Supervisor: John S. Lewis

Title: Associate Professor of Geochemistry and Chemistry

Table of Contents

1. Introduction

The planets of our solar system were formed about 4.6 billion years ago. Upon accretion the interiors of the planets heated up, releasing volatiles to the surfaces. The composition of these gases changed with time, according to the oxidation state of their source and of the material through which they passed on their way to the surface. The purpose of this thesis is to show how, over a range of initial assumptions, the mineralogy of the surface regions of a typical, undifferentiated terrestrial planet and its atmosphere will evolve during outgassing.

Most of the meteorites that fall on Earth today are chondrites and of these most are ordinary chondrites (Mason, 1962; Wasson, 1974). Also, most Earth-crossing asteroids are of ordinary chondrite composition (Chapman, 1976). Furthermore, the bulk composition of the Earth itself is most like an H chondrite, with slightly more metallic iron (Larrimer, 1971; Fig. 1). According to Lewis' (1972) models of planetary accretion the compositions of the planets are highly dependent on the temperature conditions in the primordial solar nebula at which they formed, and the temperature is in turn a strong function of distance from the Sun (Cameron, 1973). Ordinary chon-

drites in his models were formed in the vicinity of the Earth's orbit, while the carbonaceous chondrites, which contain more volatiles, formed under colder conditions, beyond the orbit of Mars. Therefore, a planet like the Earth, for instance, can be considered to have accreted mostly from ordinary chondrite material that existed in the vicinity of its orbit, with a small amount (a few percent) of material sampled from further out (Cox et al., 1978; Cox and Lewis, 1979). The dynamical models by Cox show that there is no need to invoke models in which discrete events occurring over a short period of time, such as veneering, are necessary.

Anders and Owen (1977), in order to explain the abundances of magnetite and volatiles in the Earth, have proposed an inhomogeneous accretion model in which the Earth accreted most of its present-day mass from ordinary chondrite material and was then veneered by carbonaceous chodrite material. This model is based on calculations by Weidenschilling (1975), which show that small carbonaceous chondrite objects between the orbits of Mars and Jupiter could have been perturbed by Jupiter into Mars- or Earth-crossing orbits or out of the Solar System. Anders and Owen go on to determine an exact mixture of seven various chondrite types to account for the volatile

content of the Earth. This model thus has no predictive capabilities for the other terrestrial planets. Furthermore, it assumes that the carbonaceous chondrite objects were perturbed into the vicinity of the Earth at the end of its accretion and fails to explain why the present flux of meteorites on Earth is mostly ordinary chondrites. (If the carbonaceous chondrite objects had been perturbed into Earth's orbit before the Earth finished accreting, accretion would have been homogeneous anyway). The isotopic compositions of hydrogen, nitrogen, and carbon on the Earth resulting from this model do not agree with the isotopic abundances on Earth today (Lewis et al., 1979), which happen to resemble most closely ordinary chondrites. In fact, the isotopic abundances in Anders' and Owen's model agree most closely with C3 chondrites.

Another problem with Anders' and Owen's seven-component model is that it attempts to explain the bulk composition of nine different planets and satellites (Mercury, Venus, Earth, Moon, Mars, Galilean satellites); it seems dynamically unlikely that planets in the same orbital vicinity, that is, Earth-Moon and the four Galilean satellites, would have accreted from radically different mixtures and subsequently evolved differently. It is more

reasonable to assume that the differences among these bodies are due to other factors such as size or, in the case of the Galilean satellites, different temperature and pressure conditions due to Jupiter at their orbits.

Inhomogeneous accretion models have been proposed by Turekian and Clark (1969). A consequence of inhomogeneous accretion models is that very rapid ($<10^5$ years for the Earth) accretion is required to generate enough heat to melt and differentiate an iron-nickel core. If the Moon accreted inhomogeneously, it would need to accrete in less than 100 years to generate enough heat to melt and differentiate. Rapid accretion models fail totally to explain why Vesta is differentiated. Even if Vesta accreted instantaneously, its temperature would rise only $10^{\circ}K$, far from enough to melt it. Another heat source was present on Vesta, one that must have been present in the other planets as well; thus it is unnecessary to require rapid accretion to generate enough heat for melting and differentiation. Compositional studies by Lewis and Barshay (Lewis, 1972a; Barshay and Lewis, 1976) of inhomogeneous accretion models also indicate important chemical discrepancies: FeO and hydrous silicates do not form, so that the Earth is deprived of water, and each of the terrestrial planets, including Mars, should possess a

massive iron core.

Ringwood (1966), in order to explain the presence of ferric iron in the Earth's crust and upper mantle, has proposed that the Earth formed completely from Cl carbonaceous chondrite material. Cl chondrites contain no metal, little or no ferrous iron, up to 40% magnetite by weight, up to 20% water, 2-4% carbon, 0.5% nitrogen, 100 times the rare gas content of the Earth and ordinary chondrites, and sulfur in the form of sulfates and free sulfur (Mason, 1971). In fact, of all the chondrites, Cl chondrites in terms of composition are farthest from the bulk composition of the Earth (Fig. 1). Ringwood's hypothesis requires that rapid accretion occur and that most of the enormous quantity of volatiles initially present upon accretion be totally outgassed and blown catastrophically off the Earth. The Earth in this model would need to lose an amount of volatiles equivalent to one to two times the mass of Mars in order to reach its present day abundance of volatiles. Ringwood further claims that Venus but not Mars formed from carbonaceous chondrite material. However, observations (McCord and Gaffey, 1974; Chapman et al., 1975) indicate that there is carbonaceous chondrite material in the asteroid belt, which implies that Mars would also have to be carbonaceous. Thus, besides the serious problem of

explaining how Cl chondrites would be able to form under the pressure-temperature conditions of the primordial nebula at Earth's orbit to the exclusion of ordinary chondrites, it is extremely difficult to explain, without requiring catastrophic events, why the Earth would evolve thermally from Cl carbonaceous chondrite composition to, coincidentally, ordinary chondrite composition.

Ringwood (1978) has drastically altered his original Cl carbonaceous chondrite model to a model consisting of only 10% Cl carbonaceous chondrite material. However, even this model has an overabundance of volatiles as compared to the Earth and still requires massive loss of volatiles.

Mao (1974) has found experimentally that under extremely high pressure and temperature conditions such as those found near the Earth's core-mantle boundary, ferrous iron disproportionates into iron metal plus ferric iron. Early in the thermal history of the Earth the ferric iron, being incompatible with the denser, downgoing metal and sulfide melt and with the ferromagnesian silicates in the mantle, would partition into a low density silicate melt and migrate upward toward the surface. It will be shown in this thesis how magnetite will be formed from metallic and ferrous iron simply by oxidizing these two

components with H_2O included in gases traveling upward from the interior. Thus there is no need to invoke veneering or a radically different initial composition solely to explain the presence of ferric iron in the crust and upper mantle.

It is more likely that the Earth accreted homogeneously from cold, ordinary chondrite material with no more than a few percent of more volatile carbonaceous chondrite material mixed in. During the early history of the Earth the radioactive heat sources were still large. As soon as the Earth accreted to a large enough radius and the melting temperature of the Fe-FeS eutectic was reached, melting and differentiation of the interior began to occur. The Fe-FeS melt, being denser than the primitive bulk material, began to sink, releasing more heat in the process (Fig. 2). This process became autocatalytic, such that differentiation into an Fe-FeS core, a ferromagnesian silicate mantle, and a thin, SiO_2-rich crust of volatiles and other light elements occurred.

A philosophical point must be raised here. In our study of the universe, it is most desirable to apply the principle of Occam's Razor. Models that depend on highly unlikely coincidences and catastrophic events should be avoided if simpler models can achieve the same results.

The cold, homogeneous accretion model, being a closed system besides being simple, is thus the best currently available first-order model that we have to describe the histories of the planets in our solar system.

The cold, homogeneous accretion model has one other great advantage over many other models, that is, its ability to predict and quantify results that can be applied to other planets. Anders' and Owen's model, for instance, can only be applied to a planet post hoc; it is powerless in its ability to predict the composition and evolution of other planets.

There are two extreme mechanisms for outgassing: vulcanism and percolation. If a gas percolated upward from a deep magma layer, it would more or less reach equilibrium with the surrounding minerals as it traveled upward, depending upon its rate of ascent. If a gas erupted upward from a deep magma layer and were ejected volcanically, it would equilibrate only with the atmosphere and the near-surface layer. Both processes occur at one time or another in a planet's history; determining to what extent each of these affects the compositions of the crust and atmosphere and at which points in a planet's evolution is a key to understanding the formation of an atmosphere.

2. Procedure and Results

Five different chondritic compositions were analyzed. These compositions are: H-chondrite, 99% H-chondrite + 1% Cl-chondrite, 98% H + 2% Cl, 95% H + 5% Cl, 90% H + 10% Cl. The elements, gases, and minerals considered are presented in Table 1 and the mineralogy of each of the five assemblages is presented in Tables 2-6.

An IBM 360 computer, maintained by the Laboratory for Nuclear Science at M.I.T., was used to construct models of planets of each of the above compostions and to aid in chemical calculations. The Fortran IV language was utilized for all programming.

The initial conditions were homogeneous composition, a primordial thermal gradient based on abundances of U^{238}, U^{235}, Th^{232}, and K^{40} 4.6 billion years ago, a radius of 6000 km., and a surface temperature of 278°K.

The abundances of the long-lived radionuclides 4.6 billion years ago were determined by solving the following equation:

$$N_i = N_{io} e^{-\lambda_i t}$$

where $\lambda_i = \frac{\ln 2}{t_{1/2_i}}$

$t_{1/2_i}$ = half-life of component i

t = 4.6 billion years

N_i = present abundance of component i

N_{io} = abundance of component i 4.6 billion years ago.

The thermal gradient was then obtained from the equation:

$$\frac{dT}{dz} = \frac{A}{K}$$

where K = thermal conductivity = 4.5×10^{-3} cal/sec-cm-^{o}K

A = heat flow

and was determined to be about 20^{o}K/km.

The outer layer of each model planet was divided into 21 layers, each 3 km. thick, much like an onion, such that a range of temperatures from 308^{o}K to 1508^{o}K was considered (Fig. 3). The temperatures at which chemical equilibrium calculations were done were those in the middle of each layer. Thermodynamic data were drawn from the Janaf tables and those compiled by Robie and Waldbaum (1978). The lithostatic pressure of each layer was considered to be a simple function of density and the gravitational acceleration at the corresponding radius, assuming an uncompressed, homogeneous body; that is, $P_{lith.} = \rho g z$

where ρ = density, g = gravitational acceleration

z = depth inside the planet

The average, uncompressed density of the planet was taken to be 3.7 gm/cm^3.

Studies of Earth rocks by Brace et al. (1972) and by Brace and Orange (1968) have shown that the pore volume ranges from 10^{-2} to 10^{-4} cm^3 per cubic centimeter of rock. Chondrites also exhibit the same range of pore volumes (Alexeyeva, 1958). The pore volume in this thesis was assumed to be 10^{-3}.

The initial equilibrium assemblage at the temperatute and pressure conditions in the middle of each layer was then calculated, using sets of simultaneous mass balance and equilibrium equations. Ideality was assumed throughout. The solid solutions considered were:

Iron-nickel-graphite-nitrogen	(Metal)
Forsterite-fayalite	(Olivine)
Enstatite-ferrosilite	(Pyroxene)
Albite-anorthite	(Feldspar).

The activity of each of the above components (with the exception of nitrogen and graphite; see below) was considered to be the mole fraction of that component in its solution, such that the activity of each solution was always 1 if at least one of its components existed. Orthoclase was assumed to be a separate phase with

activity = 1, not included in the feldspar solution.

The solubility of nitrogen in iron metal at high temperatures, according to Sievert's Law, was taken into account. Sievert's Law states that

$$[N] = K(P_{N_2})^{1/2}$$

where [N] = concentration of nitrogen in the metal and K is obtained from Fig. 4.

The activity of graphite was taken to be a function of its concentration in the metal (Lewis et al., 1979), according to the equation

$$\log A_{gr} = \log PPM_{gr} + (2300 + 2000XF_{Ni})/T + .3XF_{Ni} - 6.24$$

where A_{gr} = activity of graphite

PPM_{gr} = parts per million by weight of graphite in the metal

XF_{Ni} = mole fraction of nickel in the metal

T = temperature

The initial equilibrium gas composition of each compositional model is presented in Figures 5-9. Each mineralogical assemblage is dominated by N_2 at low temperatures and by CH_4 above about 430°K. Note the non-linear behavior of N_2 at 1200°K due to Sievert's Law and the non-linear behavior of HCl at high

temperatures. Talc is stable only in layers 1 - 3; the phase change from talc-forsterite-enstatite to forsterite-enstatite accounts for the discontinuities of the hydrogen-bearing gas curves at layer 4.

The initial mineralogical equilibrium assemblage of each layer for each chondritic model is presented in Figures 10-14.

Table 7 lists the sequence of mineralogical changes as outgassing progresses; the sequence is the same for each of the five assemblages considered.

The time-dependent evolution of talc, forsterite, fayalite, iron metal, and magnetite is presented in Figures 15-19.

The behavior of each of the components in solid solution is as follows:

Feldspar

Albite and anorthite exist in solution with each other during the initial sequence of outgassing steps. As oxidation of the layer progresses, nepheline and muscovite become stable according to the reactions:

$$NaAlSi_3O_8 = NaAlSiO_4 + 2SiO_2$$

$$KAlSi_3O_8 + CaAl_2Si_2O_8 + MgO + H_2O = KAl_3Si_3O_{10}(OH)_2 + CaMg(SiO_3)_2$$

The activity of anorthite reaches 1 when the albite is depleted. Muscovite forms rapidly until the orthoclase is depleted; part of the anorthite is used up in the reaction to form muscovite + diopside (added to the diopside present initially).

Olivine

As can be seen from Figures 15-19, forsterite and fayalite achieve a steady state fairly rapidly. When the activity of iron metal becomes less than 0.5, fayalite begins to be oxidized into magnetite together with the iron metal until both the iron and the fayalite are depleted. At the same time, talc and forsterite increase slightly in abundance to accomodate the SiO_2 released upon fayalite depletion.

Pyroxene

Ferrosilite becomes stable in layer 4 ($488^{o}K$) in all of the assemblages considered. Enstatite exists initially in the surface layer of each assemblage except for 90%H + 10%Cl, but gets rapidly depleted into talc + forsterite as hydrogen and oxygen are introduced into the layer with each step.

Metal

The activities of nickel and iron metal remain fairly constant throughout most of the outgassing sequence, due to the much greater molar abundance of

iron relative to nickel. The activity of iron begins to decrease rapidly toward the end of the outgassing sequence and the avtivity of nickel approaches 1 as the iron and fayalite disappear.

Table 8 lists the composition of the 'raw' atmosphere of each model at the final step considered. Methane is dominant throughout the outgassing sequence as long as iron metal is present in the surface layer. Atmospheric escape of hydrogen, interactions with the surface layer, and other atmospheric processes were not considered; table 8 is merely a listing of the gases pumped out of the surface layers of the outgassing models.

3. Summary and Proposals for Further Research

The results presented in this thesis are for only one set of initial temperature-pressure conditions, specifically, a model of the early Earth; the main purpose of the thesis was to analyze the thermodynamics of equilibrium outgassing. Future research in this area, besides investigating further the evolution of the surface regions of an outgassing planet, will take into account different sets of initial conditions.

A simple model of vulcanism, that is, outgassing from the 1208^{o}K layer directly into the surface layer, has been presented here. Percolation can also be modeled fairly simply. A model can be set up such that when the equilibrium composition of each layer has been calculated, the resulting gas in each layer is moved upward to the next layer and reequilibrated. (An infinite gas reservoir below the bottommost layer is assumed). Preliminary calculations indicate that the evolution of the surface layers up to about 450^{o}K and atmosphere will not be much different from the volcanic model.

The lithostatic pressure is a direct function of radius; the radius of the model presented here is, needless to say, the upper limit for terrestrial planets in our solar system. With a smaller radius, if the thermal

gradient is steep enough, it is possible that gas vulcanism from unmelted high temperature layers could occur, since the lithostatic pressure would be less than the gas pressure. Of course, the gas pressure is also dependent on volatile content; a planet composed of carbonaceous chondrite material will outgas more violently than a planet composed of ordinary chondrite material.

The temperature of each layer in the model presented here is a function only of long-lived radionuclides and the surface temperature. Future models will take into account the heat produced by accretion and gravitational infall of denser material toward the core. Again, a higher thermal gradient will induce more outgassing.

The sequence of mineralogical changes up until the depletion of iron metal has been investigated here. Further outgassing will continue to oxidize the surface regions until eventually the gas pumped into the atmosphere will be oxidizing. Serpentine becomes stable when the iron metal is depleted. When all of the forsterite is depleted and the talc-serpentine buffer is reached, troilite will begin to be oxidized into magnetite plus pyrite. Nickel sulfide was not considered here; however, millerite (NiS) is believed to be stable once much of the iron metal is depleted. Calcium and magnesium sulfates will become stable when the troilite is depleted, as will liquid water. As the oxygen fugacity increases, hematite will

eventually form until the magnetite is depleted.

Applications of these outgassing models to the terrestrial planets and satellites should yield very interesting results. Venus can be modeled roughly as an ordinary chondrite with 10^{-4} times the abundance of water found in ordinary chondrites (Lewis, 1970). Such a compositional model is expected to be much more oxidizing than a hydrogen-rich mineralogical assemblage. Application to the Moon may provide clues as to whether a co-accretional model with the Earth is viable. A modest amount of water in an ordinary chondrite model of the Moon may oxidize all of the iron metal into ferrous oxide; any atmosphere produced by outgassing on the Moon would be lost to space due to the Moon's feeble gravitational field. Mars may be modeled as a C3 chondrite (Anders and Owen, 1977); the outgassing results are expected to be much the same as that of the 10%Cl-90%H model with a greater abundance of carbon. Closer investigation of the sulfur chemistry of volatile-rich models is expected to provide many insights into the outgassing process on Io. Io is very oxidized due to atmospheric escape of hydrogen from dissociation of outgasses hydrogen sulfide. In fact, it is so oxidized that elemental sulfur exists in the surface regions of the

satellite. Models of Io would have to take into consideration the tremendous gravitational attraction of Jupiter, a major factor in the outgassing process on Io.

Further research in this area will provide us with many more insights into the processes of outgassing and should contribute to our quest to understand the evolution of the Solar System.

Caption to Table 1: A list of the compounds and gases considered. Minerals that are stable at one time or another are listed in column A. Those marked with an asterisk do not undergo any changes from their initial abundances during the sequence of outgassing steps. The gases considered are listed in column B. Other compounds considered that never became stable are listed in column C.

Table 1

A	B	C
Mg_2SiO_4	CO	SiO_2
Fe_2SiO_4	CO_2	MgO
$MgSiO_3$	CH_4	FeO
$FeSiO_3$	H_2	$Mg(OH)_2$
*FeS	O_2	$Mg_3Si_2O_5(OH)_4$
$NaAlSi_3O_8$	H_2S	CaO
$CaAl_2Si_2O_8$	SO_2	Al_2O_3
$KAlSi_3O_8$	COS	Na_2O
$CaMg(SiO_3)_2$	H_2O	K_2O
*$Ca_3(PO_4)_2$	S_2	P_2O_5
*$Ca_5(PO_4)_3F$	N_2	NiO
*$3NaAlSiO_4.NaCl$	NH_3	Fe_2O_3
$NaAlSiO_4$	HCl	$MgCO_3$
$KAl_3Si_3O_{10}(OH)_2$	HF	$MgSO_4$
$Mg_3Si_4O_{10}(OH)_2$	Cl_2	$CaCO_3$
C	F_2	Na
Fe		
Ni		

Table 2

The initial mineralogical assemblage before equilibration of the H-chondrite model.

Mineral	Weight Percent
Mg_2SiO_4	25.7
Fe_2SiO_4	9.4
$MgSiO_3$	19.6
$FeSiO_3$	6.5
FeS	6.1
$NaAlSi_3O_8$	6.3
$CaAl_2Si_2O_8$	1.4
$CaMg(SiO_3)_2$	4.2
$Ca_3(PO_4)_2$	0.26
$Ca_5(PO_4)_3F$	0.26
$3NaAlSiO_4.NaCl$	0.14
$KAlSi_3O_8$	0.63
C	0.10
Fe^o	17.9
Ni^o	1.7
H_2O	0.05
N_2	0.005

Table 3

The initial mineralogical assemblage before equilibration of the 99%H + 1%Cl chondrite model.

Mineral	Weight Percent
Mg_2SiO_4	25.7
Fe_2SiO_4	9.5
$MgSiO_3$	19.4
$FeSiO_3$	6.5
FeS	6.2
$NaAlSi_3O_8$	6.2
$CaAl_2Si_2O_8$	1.4
$CaMg(SiO_3)_2$	4.2
$Ca_3(PO_4)_2$	0.25
$Ca_5(PO_4)_3F$	0.27
$3NaAlSiO_4.NaCl$	0.15
$KAlSi_3O_8$	0.63
C	0.13
Fe^o	17.7
Ni^o	1.7
H_2O	0.15
N_2	0.008

Table 4

The initial mineralogical assemblage before equilibration of the 98%H + 2%Cl chondrite model.

Mineral	Weight Percent
Mg_2SiO_4	25.9
Fe_2SiO_4	9.6
$MgSiO_3$	19.2
$FeSiO_3$	6.4
FeS	6.3
$NaAlSi_3O_8$	6.2
$CaAl_2Si_2O_8$	1.4
$CaMg(SiO_3)_2$	4.2
$Ca_3(PO_4)_2$	0.25
$Ca_5(PO_4)_3F$	0.27
$3NaAlSiO_4.NaCl$	0.16
$KAlSi_3O_8$	0.63
C	0.16
Fe^o	17.5
Ni^o	1.7
H_2O	0.25
N_2	0.01

Table 5

The initial mineralogical assemblage before equilibration of the 95%H + 5%Cl chondrite model.

Mineral	Weight Percent
Mg_2SiO_4	26.1
Fe_2SiO_4	9.9
$MgSiO_3$	18.4
$FeSiO_3$	6.4
FeS	6.6
$NaAlSi_3O_8$	6.2
$CaAl_2Si_2O_8$	1.4
$CaMg(SiO_3)_2$	4.2
$Ca_3(PO_4)_2$	0.24
$Ca_5(PO_4)_3F$	0.29
$3NaAlSiO_4.NaCl$	0.19
$KAlSi_3O_8$	0.63
C	0.25
Fe^o	16.9
Ni^o	1.7
H_2O	0.55
N_2	0.018

Table 6

The initial mineralogical assemblage before equilibration of the 90%H + 10%Cl chondrite model.

Mineral	Weight percent
Mg_2SiO_4	26.6
Fe_2SiO_4	10.5
$MgSiO_3$	17.4
$FeSiO_3$	6.2
FeS	7.2
$NaAlSi_3O_8$	6.1
$CaAl_2Si_2O_8$	1.4
$CaMg(SiO_3)_2$	4.2
$Ca_3(PO_4)_2$	0.23
$Ca_5(PO_4)_3F$	0.31
$3NaAlSiO_4.NaCl$	0.24
$KAlSi_3O_8$	0.64
C	0.41
Fe^o	16.0
Ni^o	1.6
H_2O	1.1
N_2	0.031

Caption to table 7: The sequence of mineralogical changes in layer 1 as outgassing progresses. Each of the mineralogical assemblages starts at step A with the exception of the 90%H + 10%Cl assemblage, which starts at step C.

Table 7

Sequence of mineralogical changes in layer 1 as outgassing progresses.

A. Enstatite, forsterite, fayalite, talc, iron metal, anorthite, albite, orthoclase

enstatite depleted

B. Forsterite,fayalite, talc, iron metal, anorthite, albite, orthoclase

nepheline, muscovite appear

C. Forsterite, fayalite, talc, iron metal, anorthite, albite, orthoclase, nepheline, muscovite

orthoclase depleted

D. Forsterite, fayalite, talc, iron metal, anorthite, albite, nepheline, muscovite

albite depleted

E. Forsterite, fayalite, talc, iron metal, anorthite, nepheline, muscovite

magnetite appears

F. Forsterite, fayalite, iron metal. talc, anorthite, nepheline, muscovite, magnetite

iron metal, fayalite disappear

G. Forsterite, talc, anorthite, neheline, muscovite, magnetite

Table 8

Composition of 'raw' atmosphere of each model after final outgassing step in terms of log of mole fraction of each gas.

Gas	H chondrite	99%H + 1%Cl	98%H + 2%Cl	95%H + 5%Cl	90%H + 10%Cl
CH_4	- 0.041	- 0.025	- 0.020	- 0.018	- 0.017
N_2	- 1.15	- 1.32	- 1.40	- 1.43	- 1.46
NH_3	- 1.70	- 1.98	- 2.21	- 2.40	- 2.56
H_2	- 4.57	- 4.97	- 5.87	- 5.90	- 5.93
H_2O	- 8.65	- 9.05	- 9.95	-10.2	-10.5
H_2S	-15.0	-15.4	-16.3	-16.6	-16.9
CO_2	-21.7	-22.1	-23.0	-23.3	-23.6
CO	-22.5	-22.9	-23.2	-23.5	-23.8
HF	-33.7	-34.1	-35.0	-35.3	-35.6
COS	-34.5	-34.9	-35.8	-36.1	-36.4
S_2	-36.9	-37.3	-38.2	-38.5	-38.8
HCl	-40.0	-40.4	-41.3	-41.6	-41.9
SO_2	-55.3	-55.7	-56.6	-56.9	-57.2
O_2	-88.6	-89.0	-89.9	-90.2	-90.5
Cl_2	-107.7	-108.1	-109.0	-109.3	-109.6
F_2	-156.1	-156.5	-157.4	-157.7	-158.0

Caption to Figure 1: Plot of Fe^{o}+FeS vs. FeO of the various chondrite types. The bulk composition of the Earth and the mean composition of the present flux of meteorites are included.

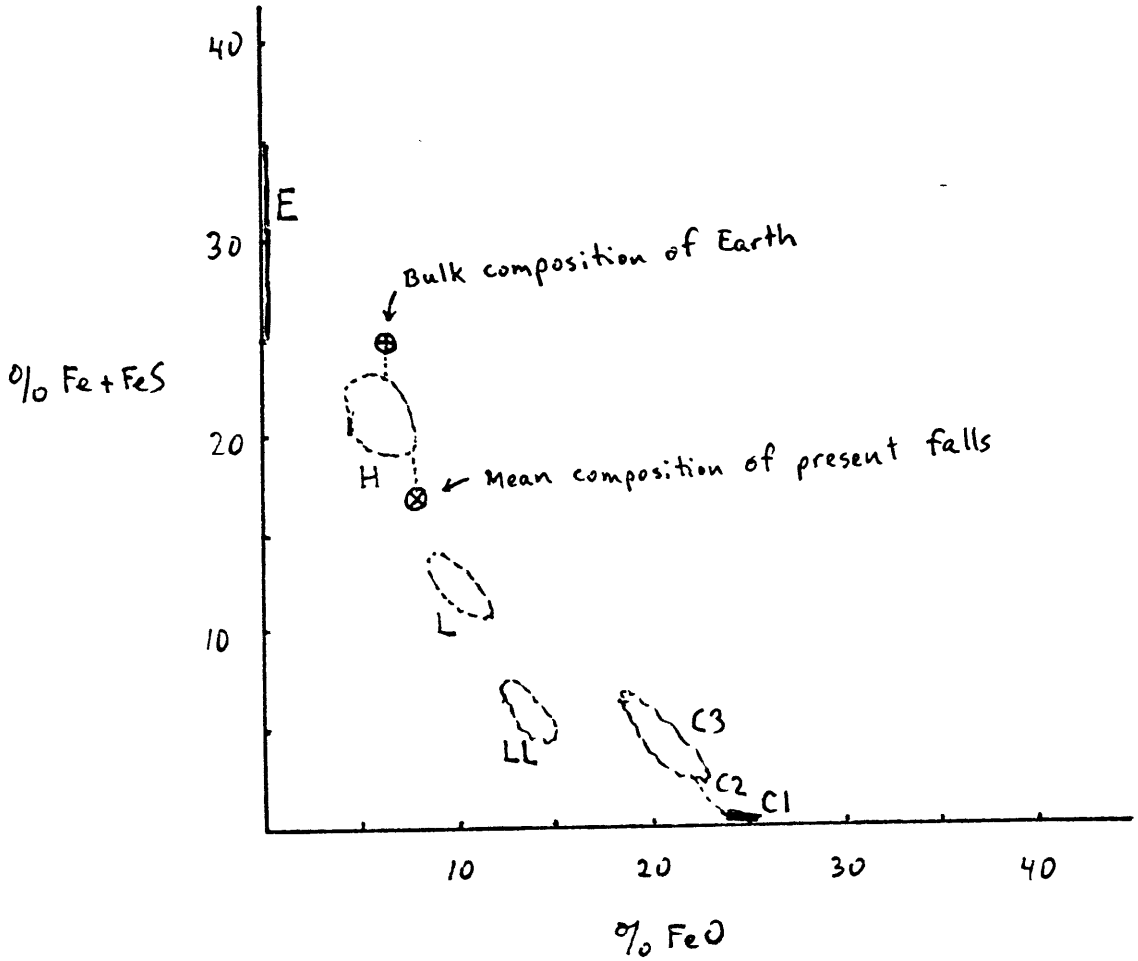
40
30
20
10
E
Bulk composition of Earth
H
Mean composition of present falls
L
LL
C3
C2
C1
10
20
30
40
% Fe + FeS
% FeO

Fig. 1

Caption to Figure 2: Plot of time-dependent evolution of temperature vs. depth of the geotherm in the early Earth. Initially the body is a cold, homogeneous mixture. As time progresses, the interior is heated up by radionuclides. When the temperature of the Fe-FeS eutectic is reached at a certain point in the interior, the Fe-FeS eutectic begins to melt and differentiate, and being denser than the surrounding minerals, begins to sink. More heat is released from the gravitational energy of the sinking process, causing runaway melting to occur.

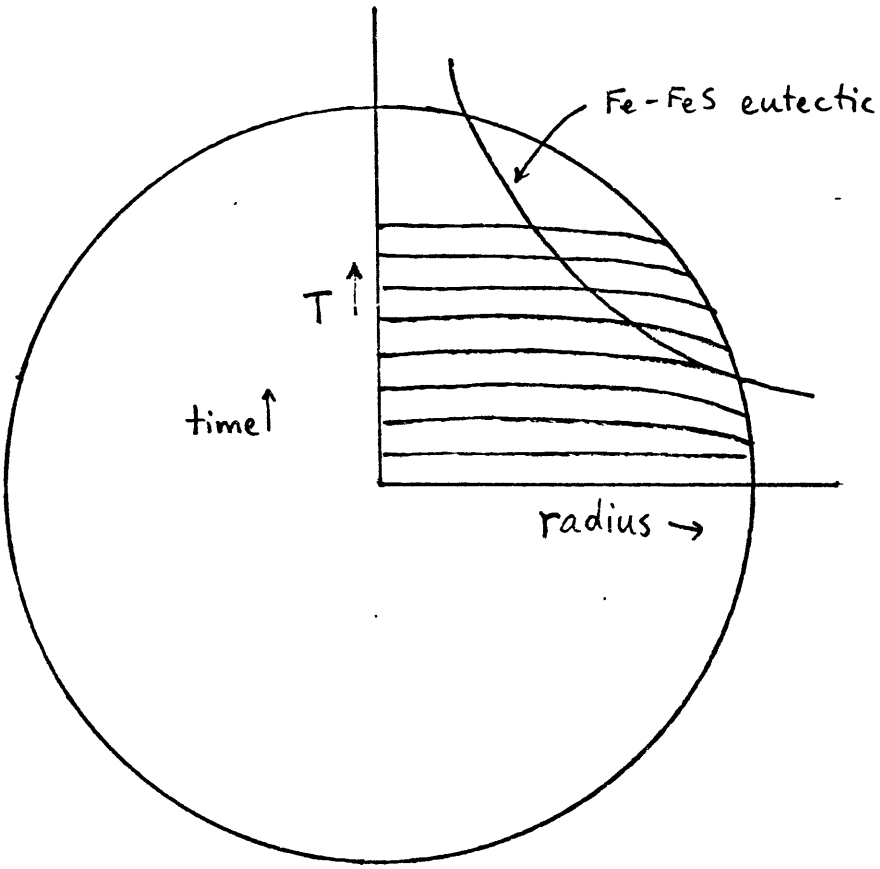

Fig. 2

Caption to Figure 3: Pie section of model planet and sketch of the surface regions. The initial equilibrium composition of each layer was calculated. Layer 16 (1208^{o}K) was chosen as the typical magma layer; the gas from layer 16 was moved up to layer 1, reequilibrated with layer 1, and then dumped into the atmosphere. An infinite reservoir of magmatic gases from layer 16 was assumed for the calculations in this thesis.

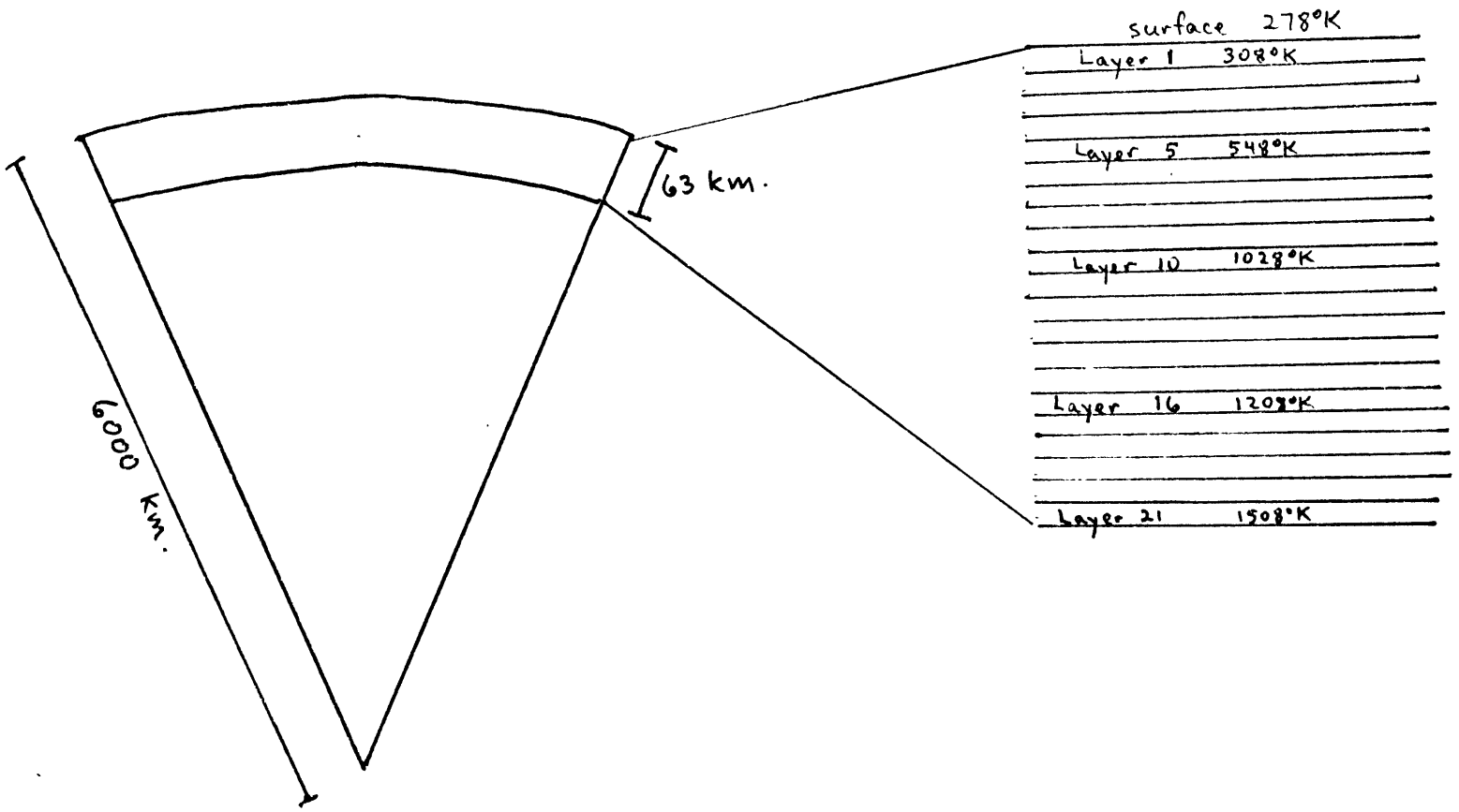
surface 278°K
Layer 1 308°K
Layer 5 548°K
Layer 10 1028°K
Layer 16 1208°K
Layer 21 1508°K
63 km.
6000 km.

Fig. 3

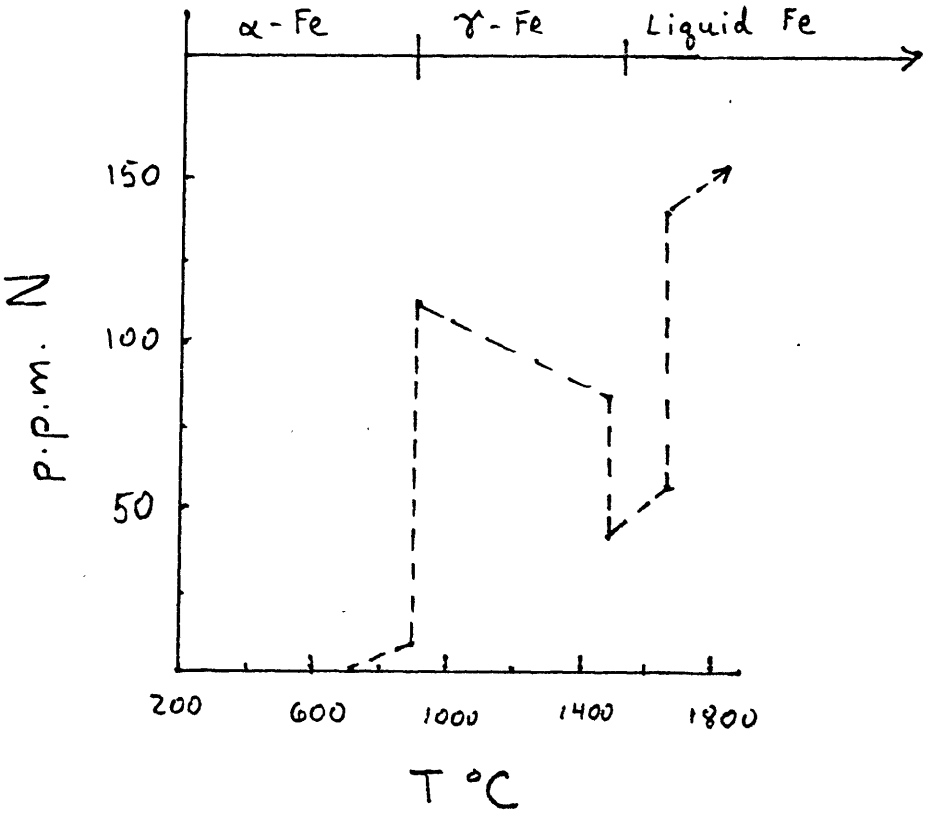

Figure 4 (after Chipman and Elliott, 1963, Fig. 16-2):

The solubility of N in different phases of iron at one atmosphere pressure.

Caption to Figure 5: The initial gas compostion of each layer of the H-chondrite model on a log P vs. -1/T plot. Note that the gas pressure in each layer is always lower than the lithostatic pressure.

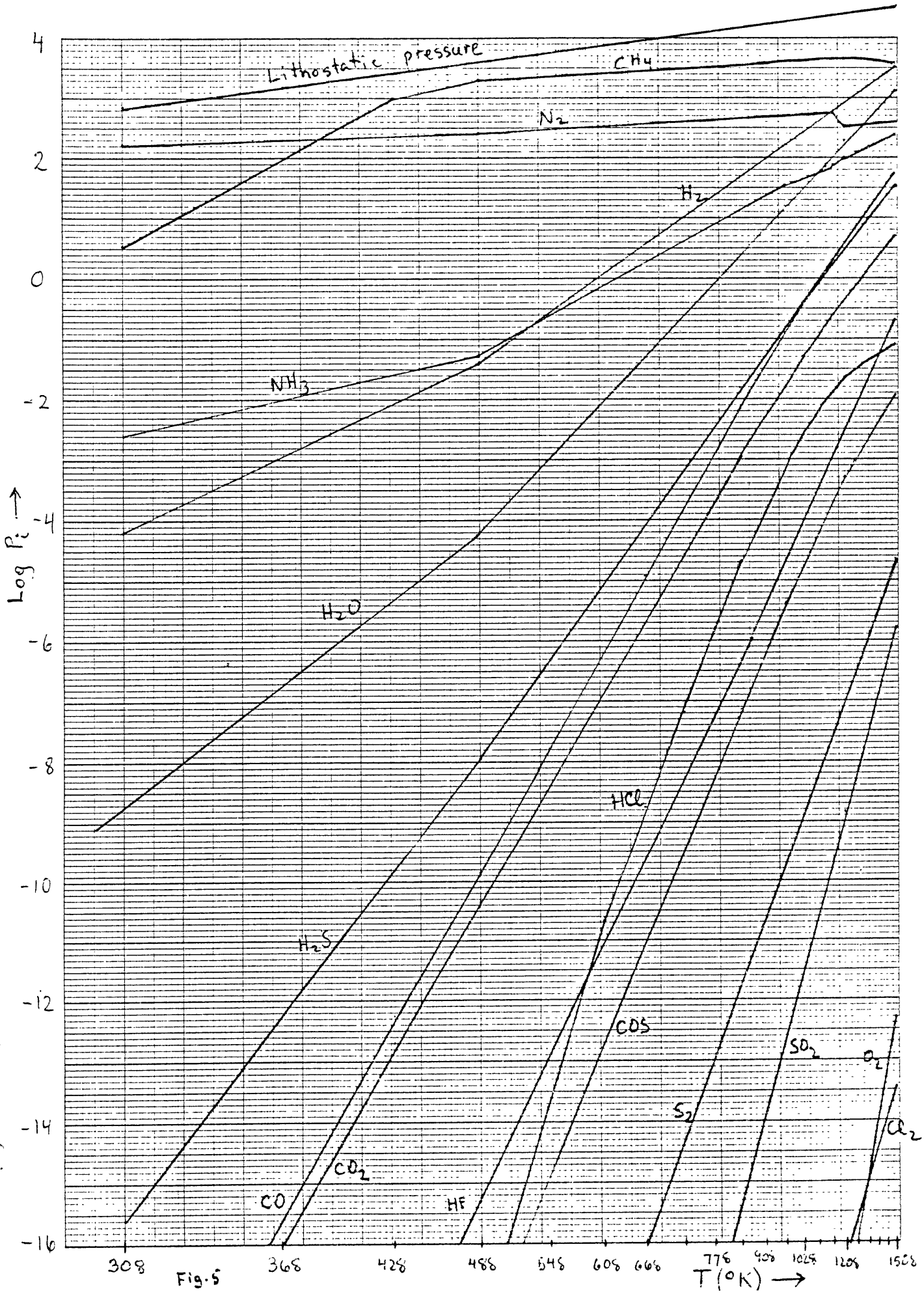

Fig. 5

Caption to Figure 6: The initial gas composition per layer of the 99%H + 1%Cl chondrite model. The gas pressure exceeds the lithostatic pressure in layers 4-6.

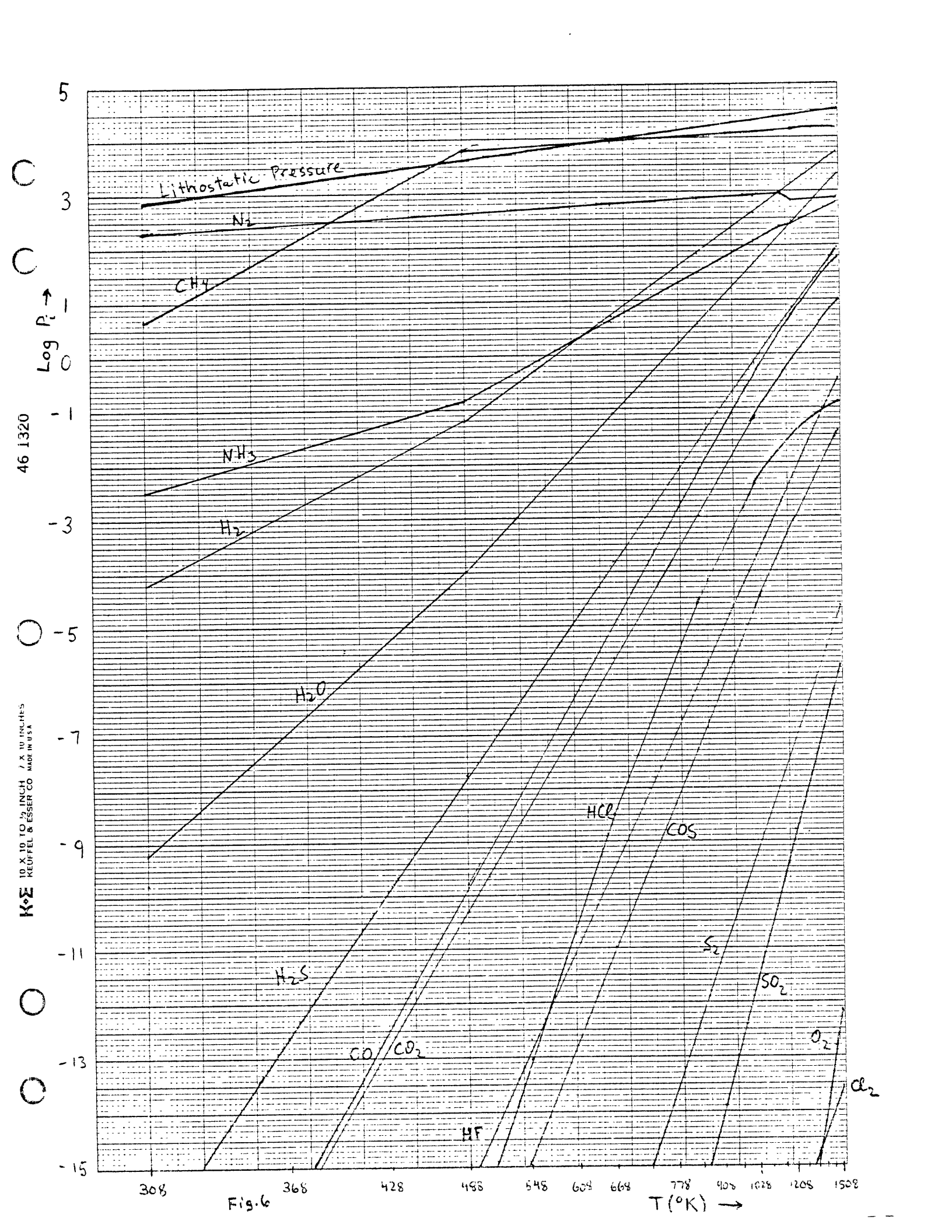

Fig. 6

Caption to Figure 7: The initial gas composition per layer of a 98%H + 2%Cl chondrite. The gas pressure exceeds the lithostatic pressure in layers 4-13.

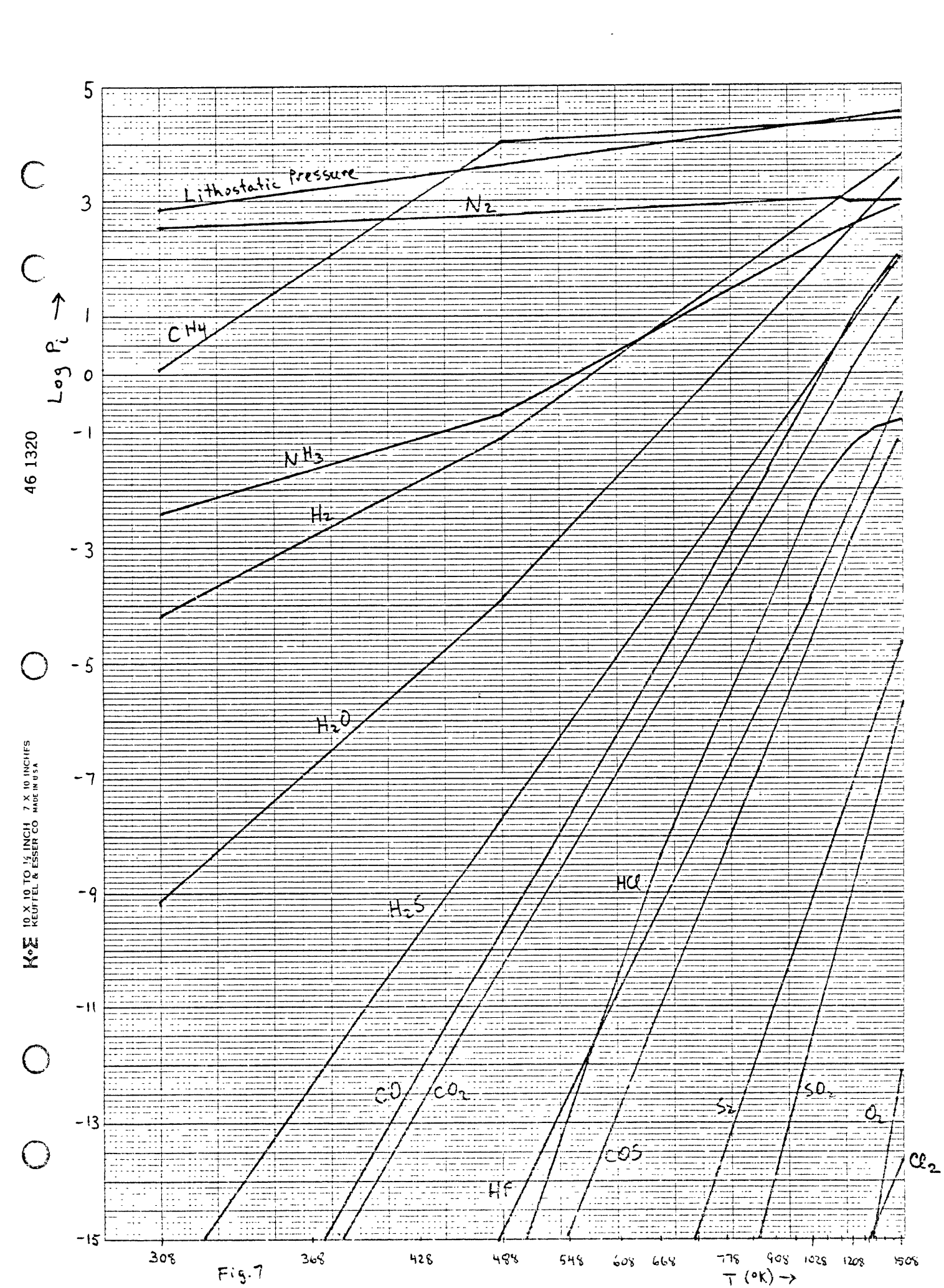

Fig. 7

Caption to Figure 8: The initial gas composition per layer of a 95%H + 5%Cl chondrite. The gas pressure exceeds the lithostatic pressure from layer 4 onward.

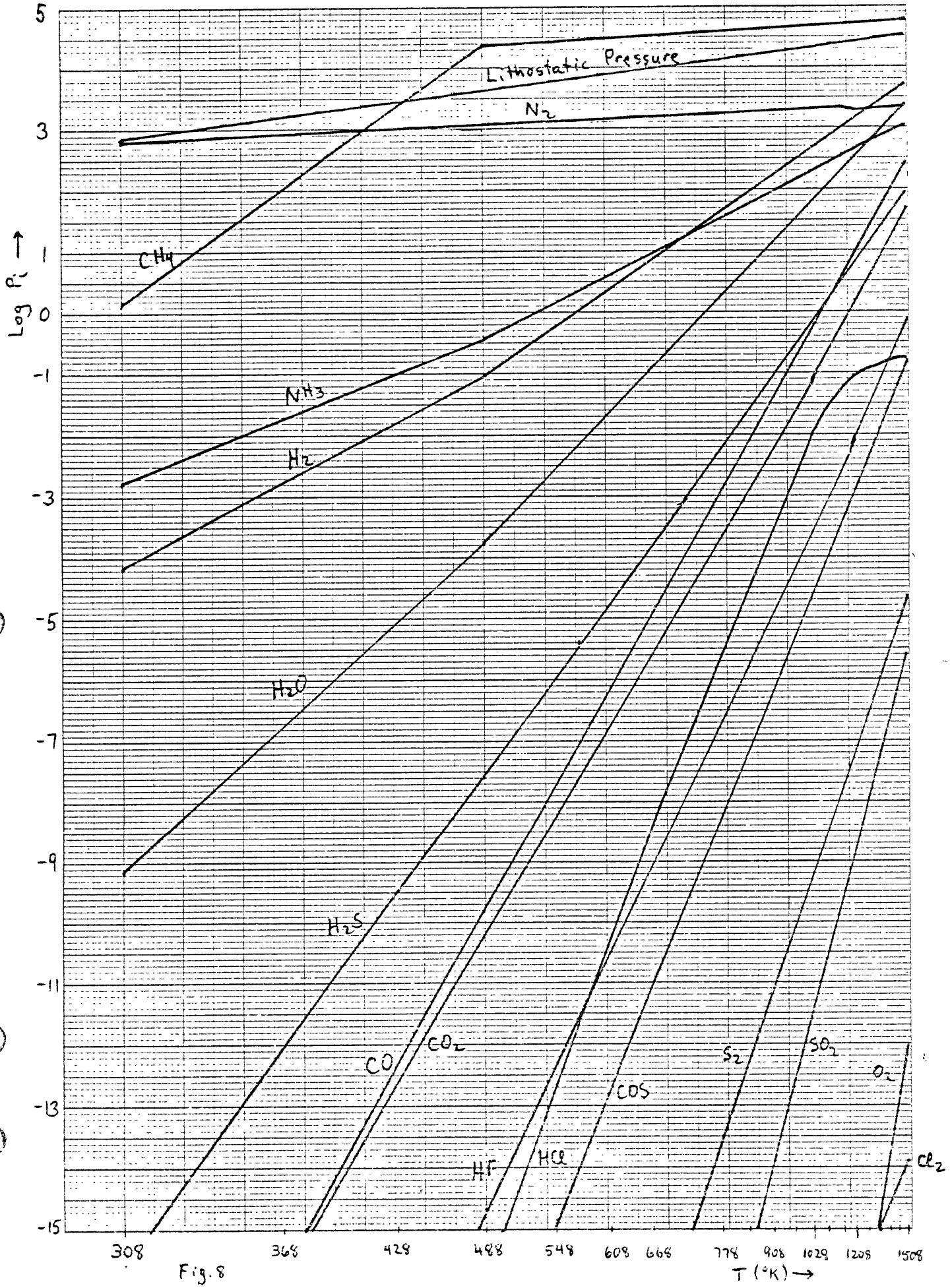

Fig. 8

Caption to Figure 9: The initial gas composition per layer of a 90%H + 10%Cl chondrite. The gas pressure exceeds the lithostatic pressure from layer 3 onward.

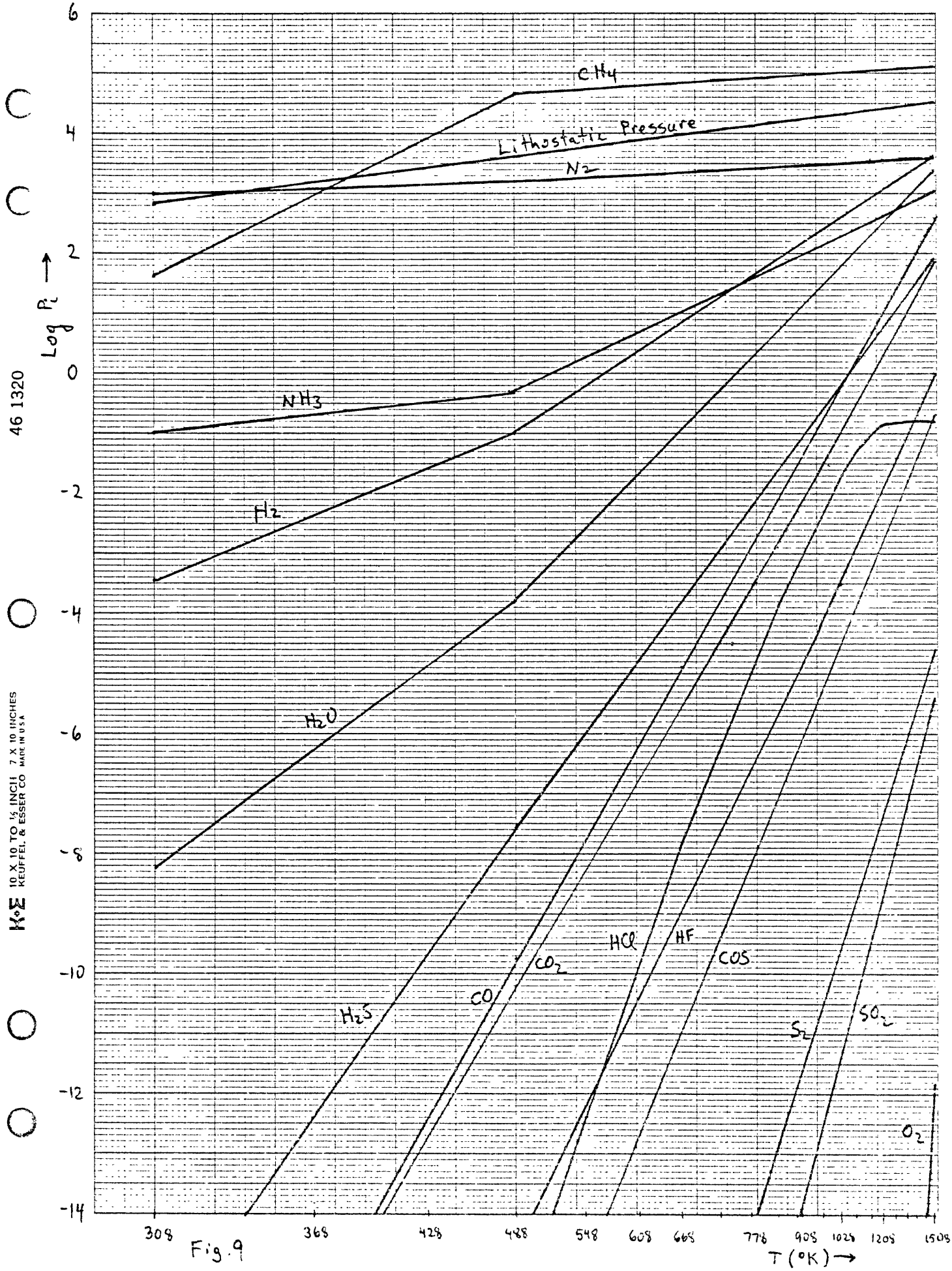

Fig. 9

Caption to Figure 10: Initial abundances of iron, forsterite, fayalite, enstatite, ferrosilite, albite, and anorthite in each layer of the H chondrite model.

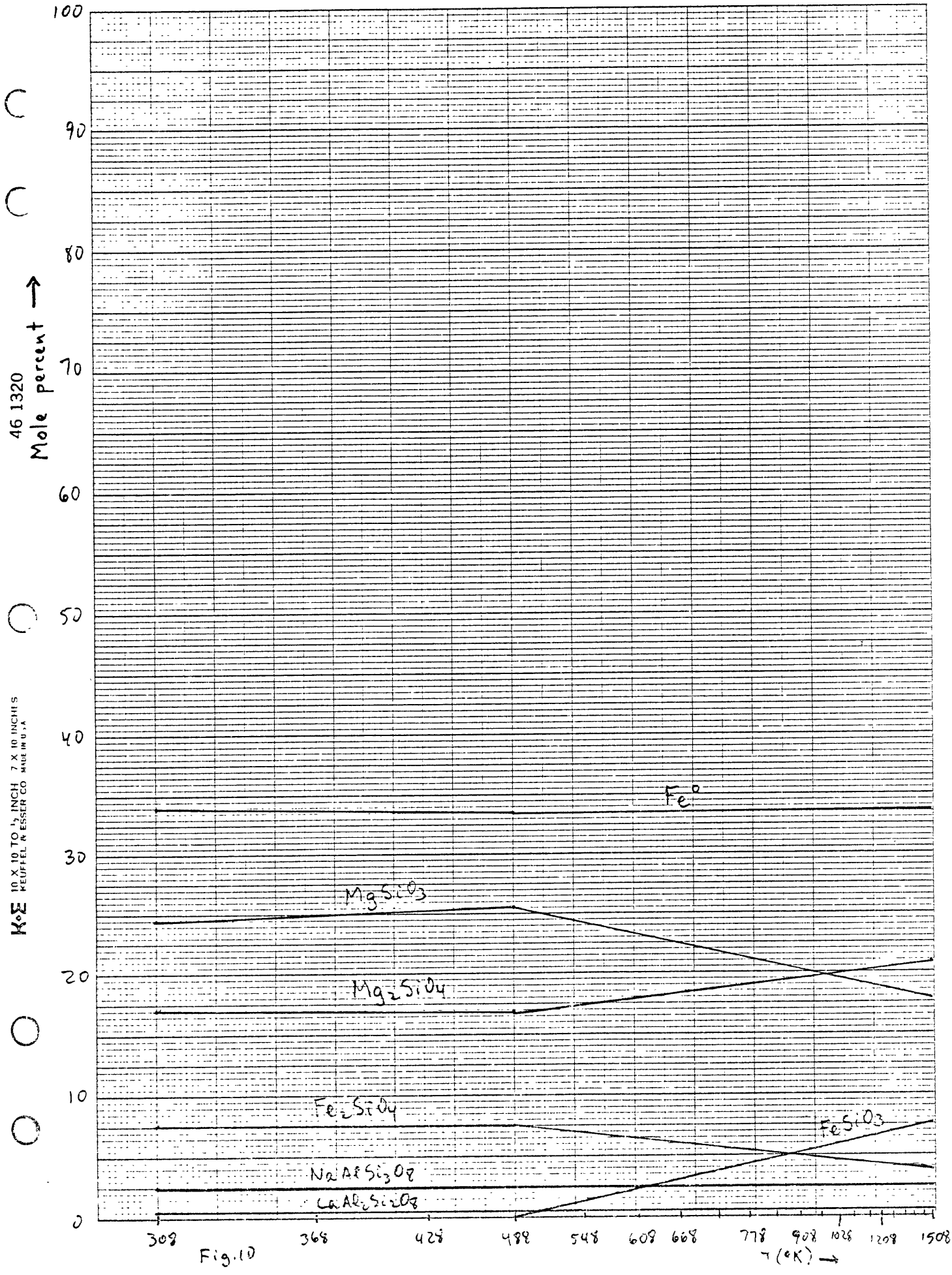
100
90
80
70
60
50
40
30
20
10
0
Mole percent →
Fe°
MgSiO3
Mg2SiO4
Fe2SiO4
FeSiO3
NaAlSi3O8
CaAl2Si2O8
308
368
428
488
548
608
668
778
908
1028
1208
1508
T (°K) →

Fig. 10

Caption to Figure 11: Initial abundances of iron, forsterite, fayalite, enstatite, ferrosilite, albite, and anorthite in each layer of the 99%H + 1%Cl chondrite model.

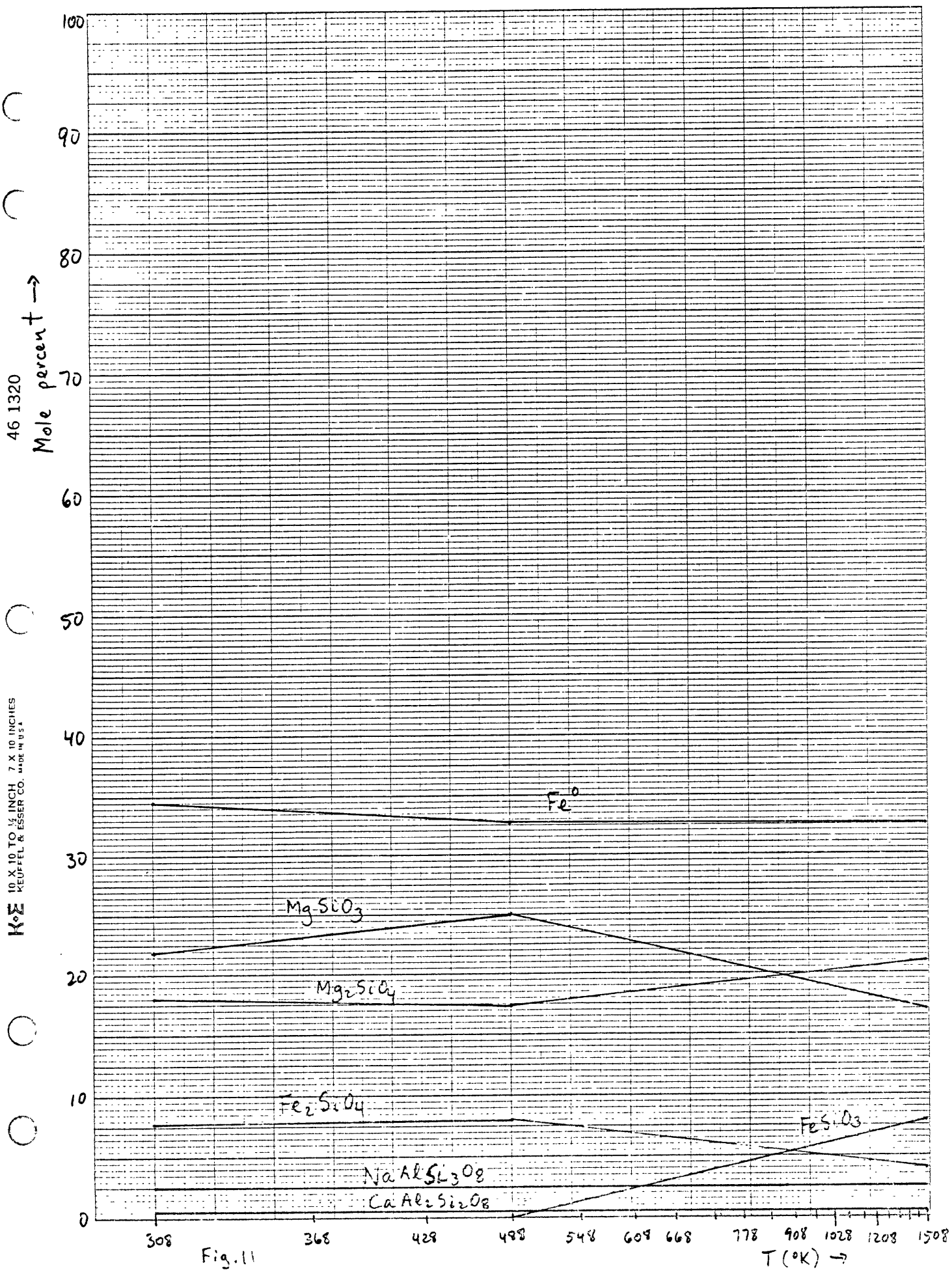

Fig. 11

Caption to Figure 12: Initial abundances of iron, forsterite, fayalite, enstatite, ferrosilite, albite, and anorthite in each layer of the 98%H + 2%Cl chondrite model.

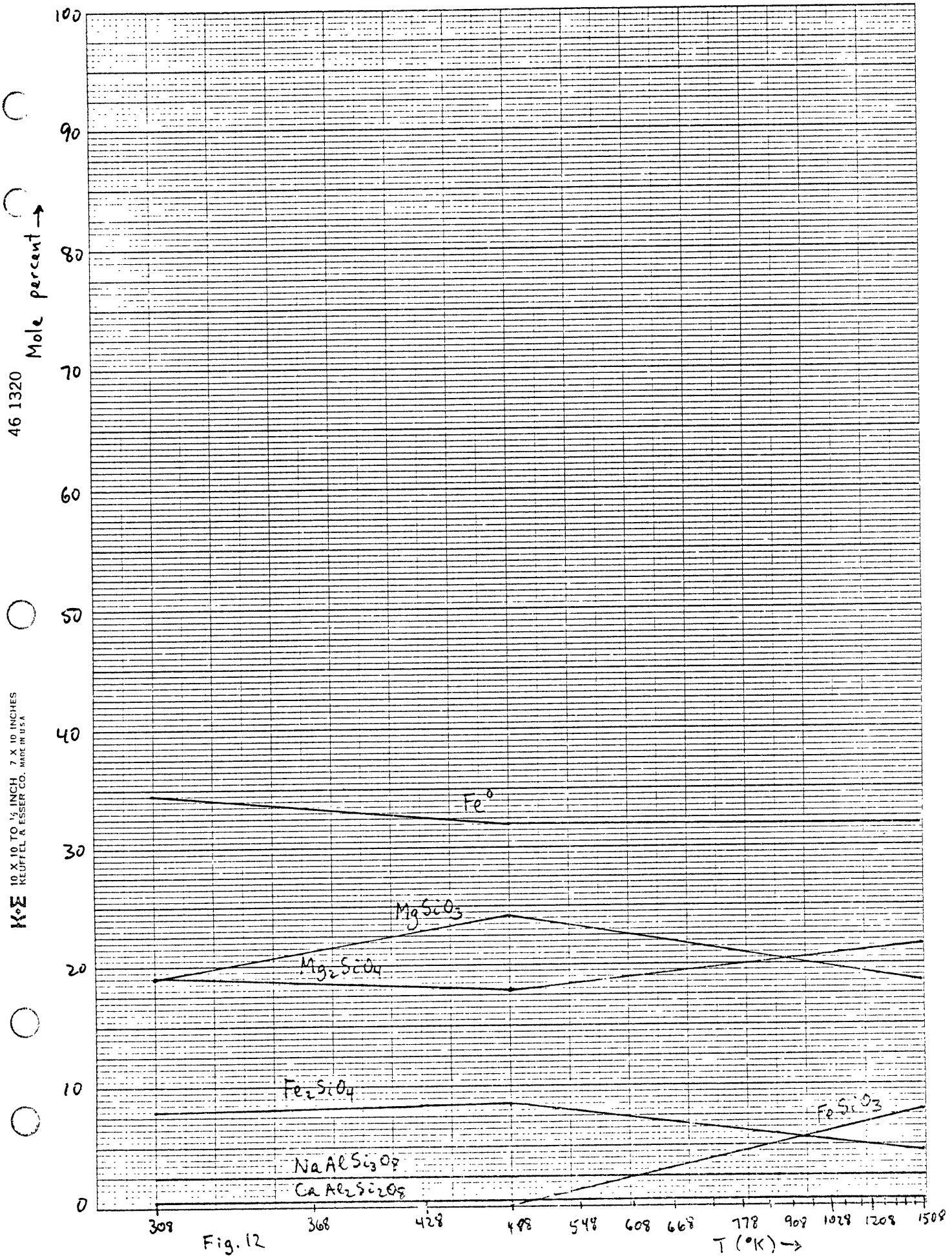

Fig. 12

Caption to Figure 13: Initial abundances of iron, forsterite, fayalite, enstatite, ferrosilite, albite, and anorthite in each layer of the 95%H + 5%Cl chondrite model.

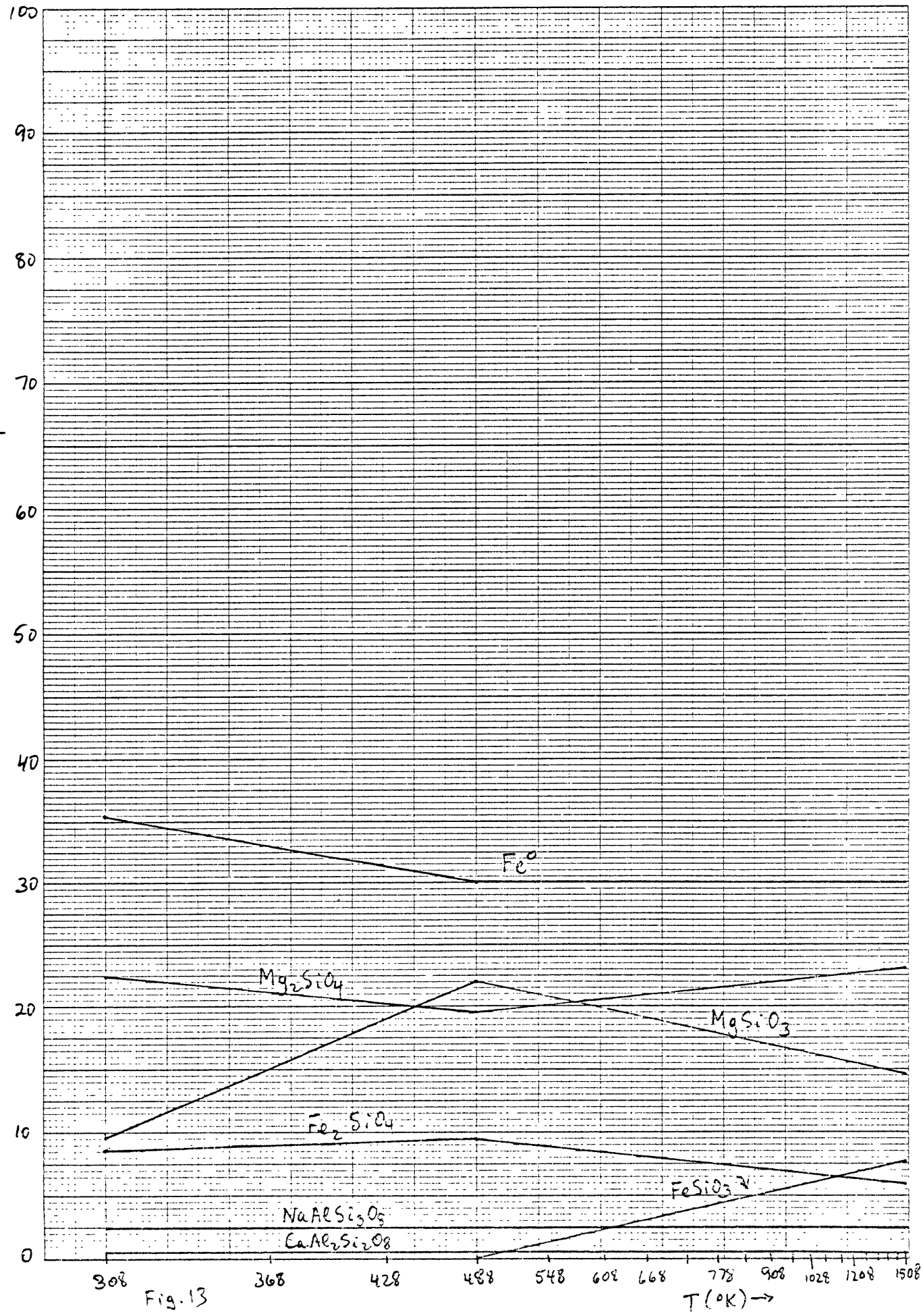

Fig. 13

Caption to Figure 14: Initial abundances of iron, forsterite, fayalite, enstatite, ferrosilite, albite, and anorthite in each layer of the 90%H + 10%Cl chondrite model.

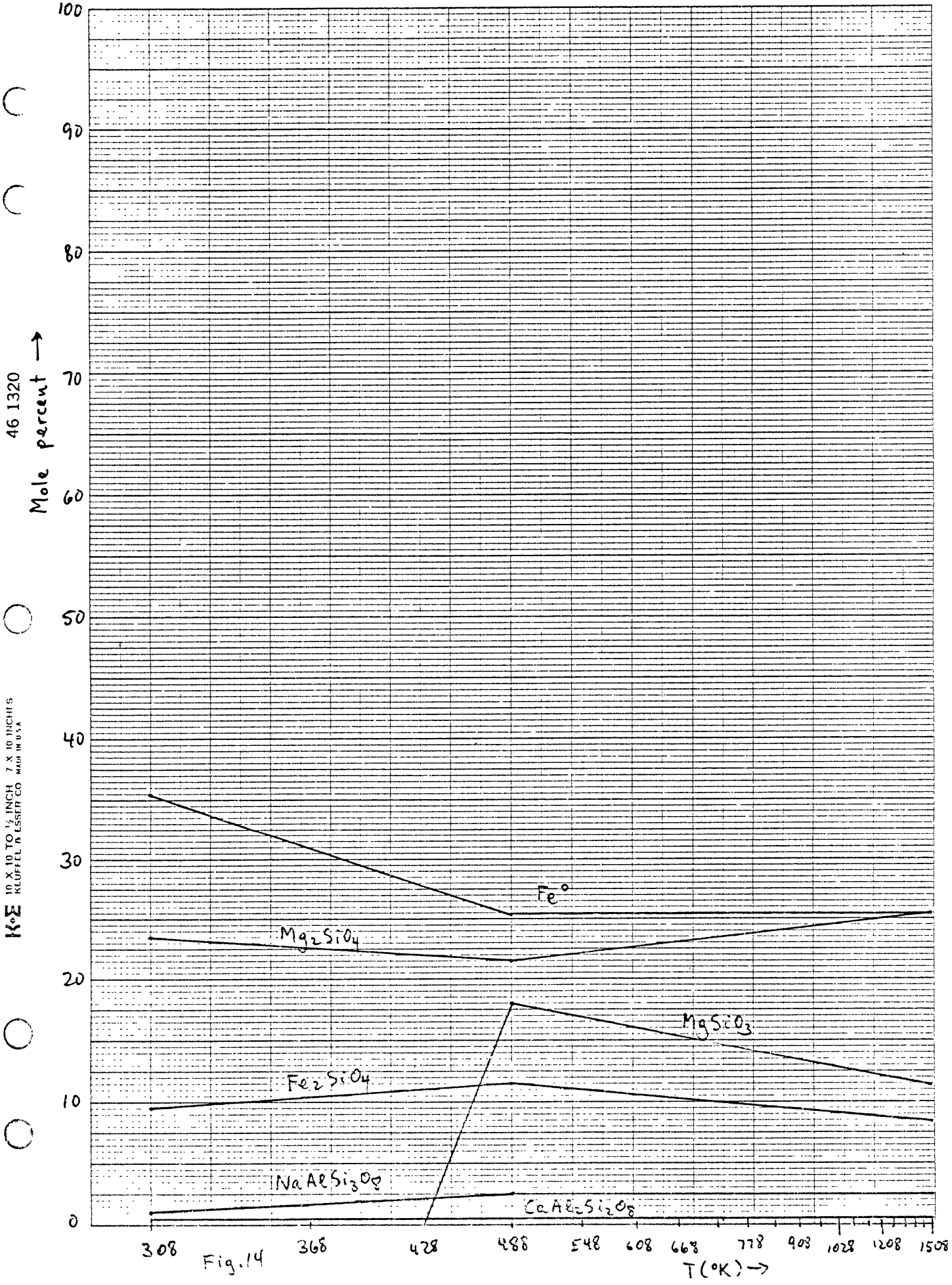

Fig. 14

Caption to Figure 15: The time-dependent evolution during outgassing of the mineralogy of the surface layer of an H chondrite planet. Note the rapid changes that occur when the magmatic gases are first pumped into the layer. The initial abundance of graphite is steadily depleted as CH_4 is produced until the only carbon in the layer is that introduced by the CH_4 from the magma layer; the carbon introduced from the magma layer remains as CH_4 and is dumped into the atmosphere. As soon as the graphite is depleted Fe_3O_4 begins to form from the progressive oxidation of Fe^o; $Mg_3Si_4O_{10}(OH)_2$, Mg_2SiO_4, and Fe_2SiO_4 achieve a steady state until the final steps when Fe_2SiO_4 begins to be depleted and together with the Fe^o is oxidized into Fe_3O_4.

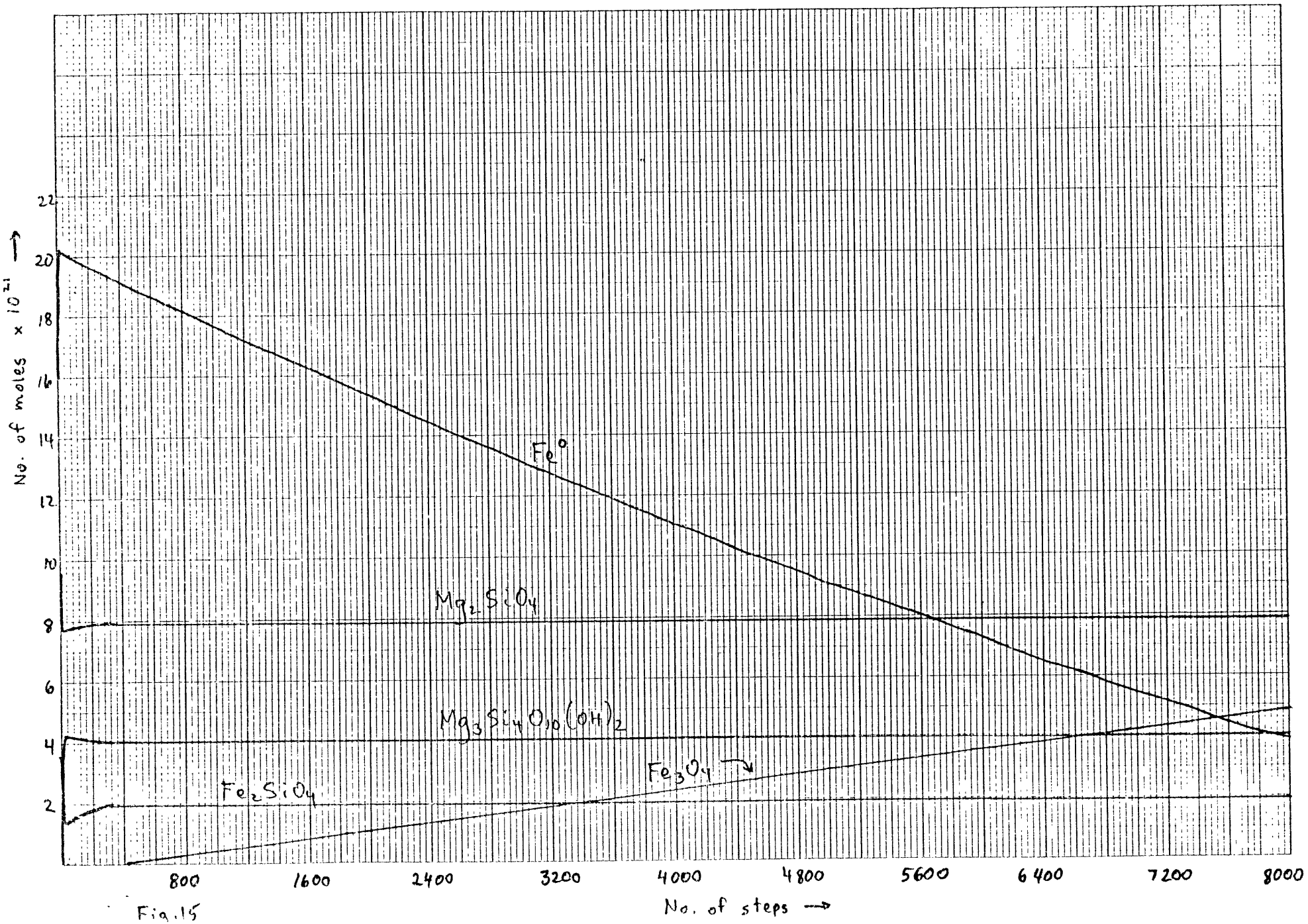

Fig. 15

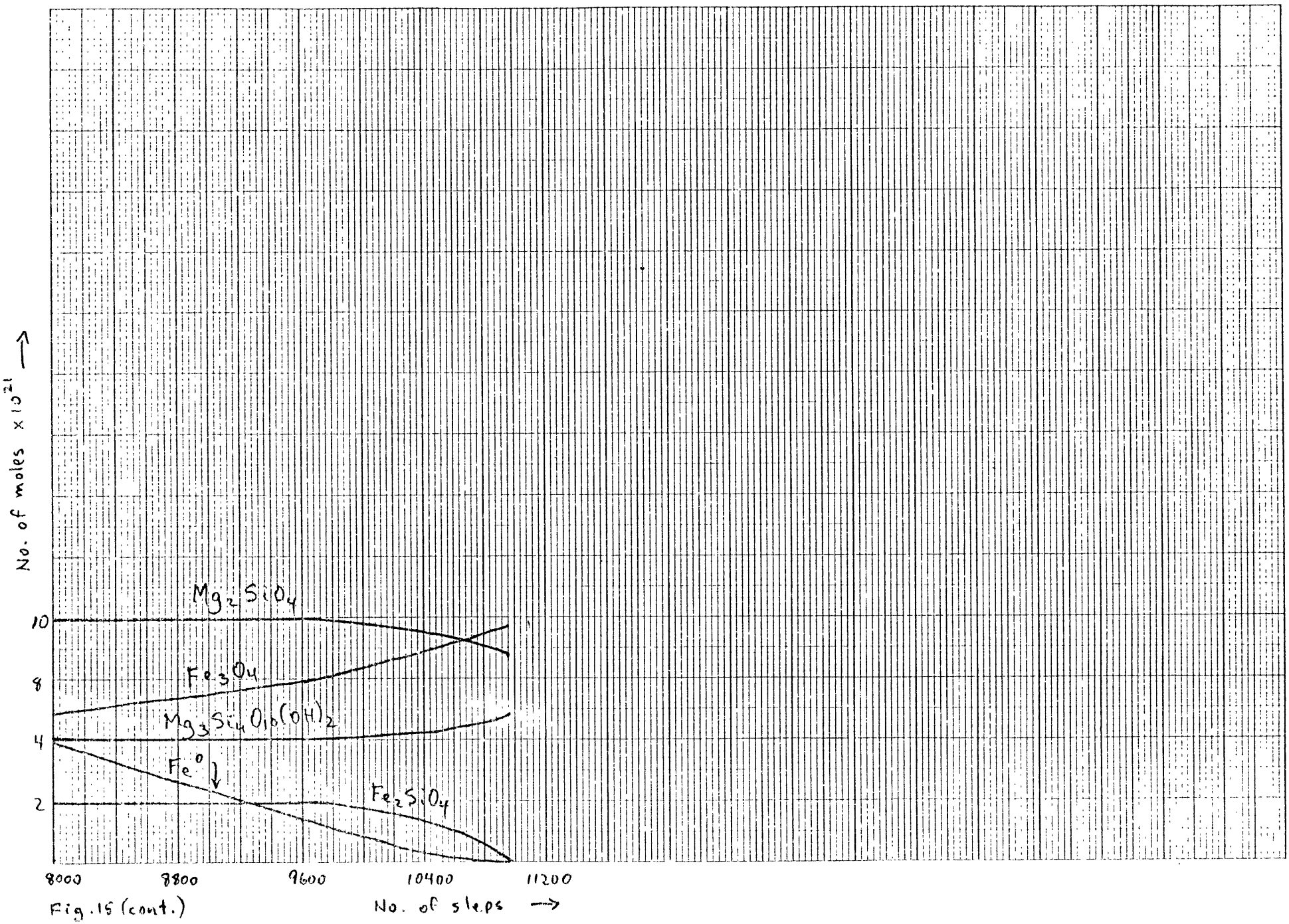

Fig. 15 (cont.)

Caption to Figure 16: The time-dependent evolution during outgassing of the mineralogy of the surface layer of a 99%H + 1%Cl chondrite planet. See caption to Fig. 15.

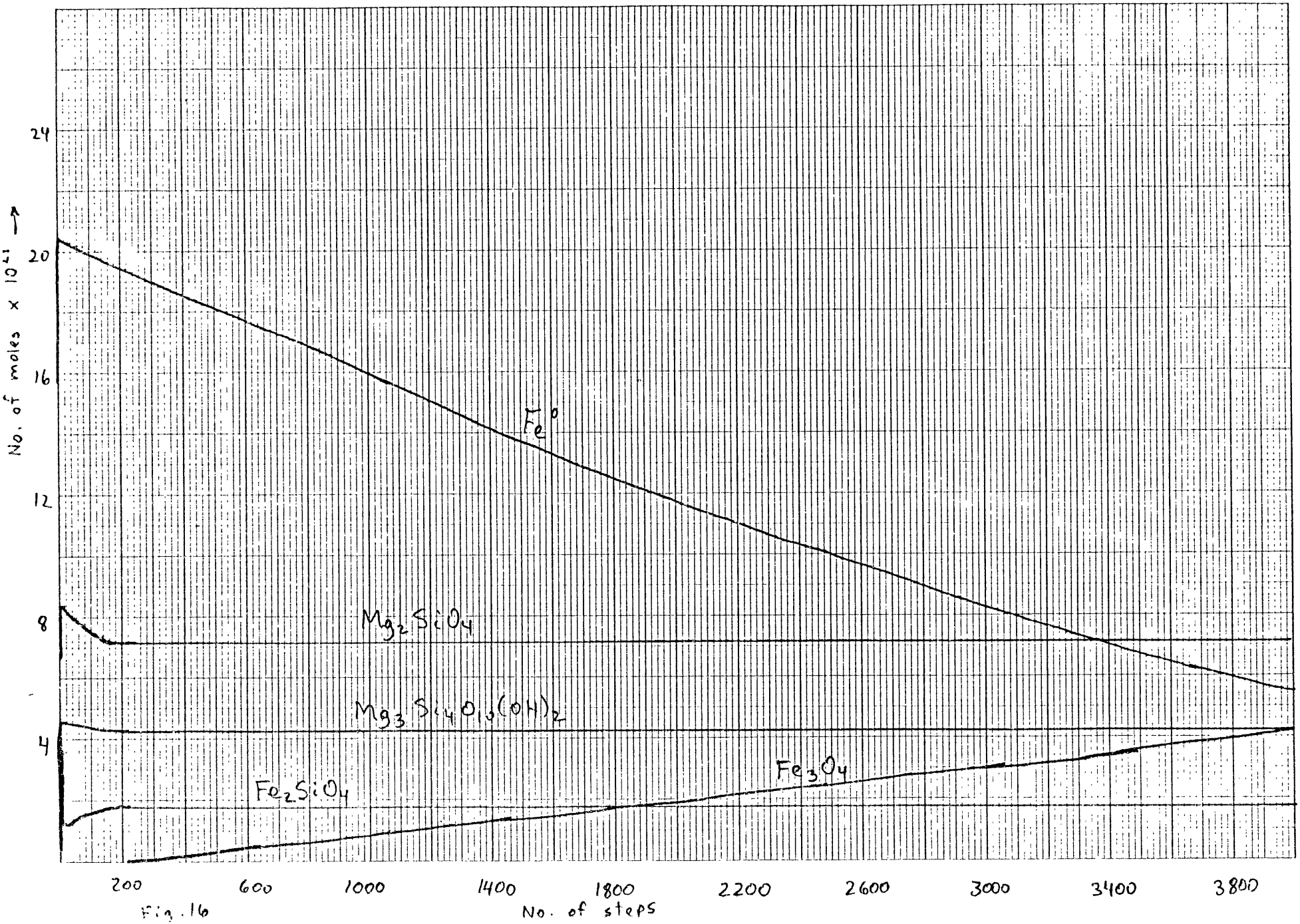

Fig. 16

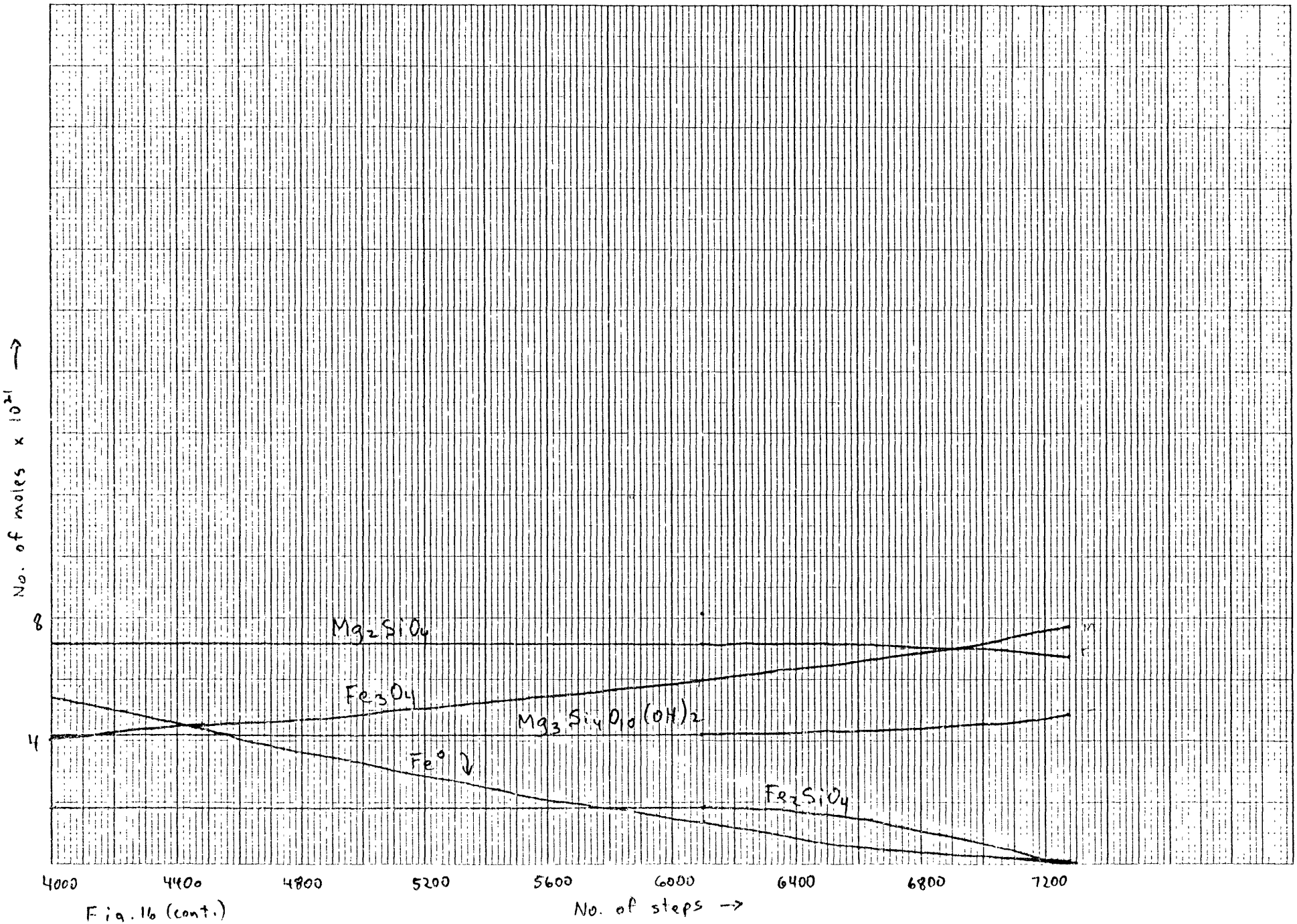

Fig. 16 (cont.)

Caption to Figure 17: The time-dependent evolution during outgassing of the mineralogy of the surface layer of a 98%H + 2%Cl chondrite planet. See caption to Fig. 15.

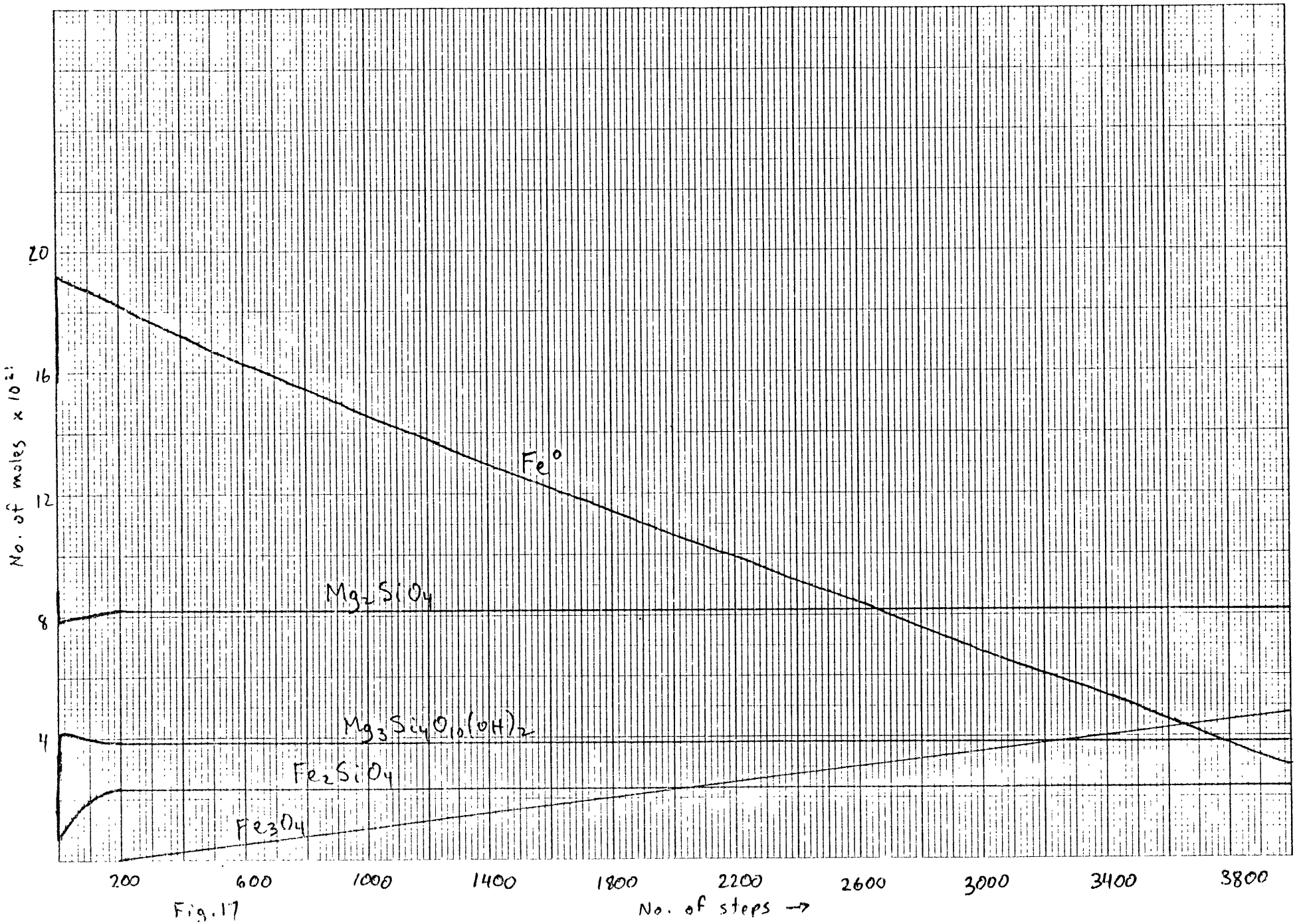
20
16
12
8
4
No. of moles x 10²
Fe°
Mg₂SiO₄
Mg₃Si₄O₁₀(OH)₂
Fe₂SiO₄
Fe₃O₄
200
600
1000
1400
1800
2200
2600
3000
3400
3800
No. of steps →

Fig. 17

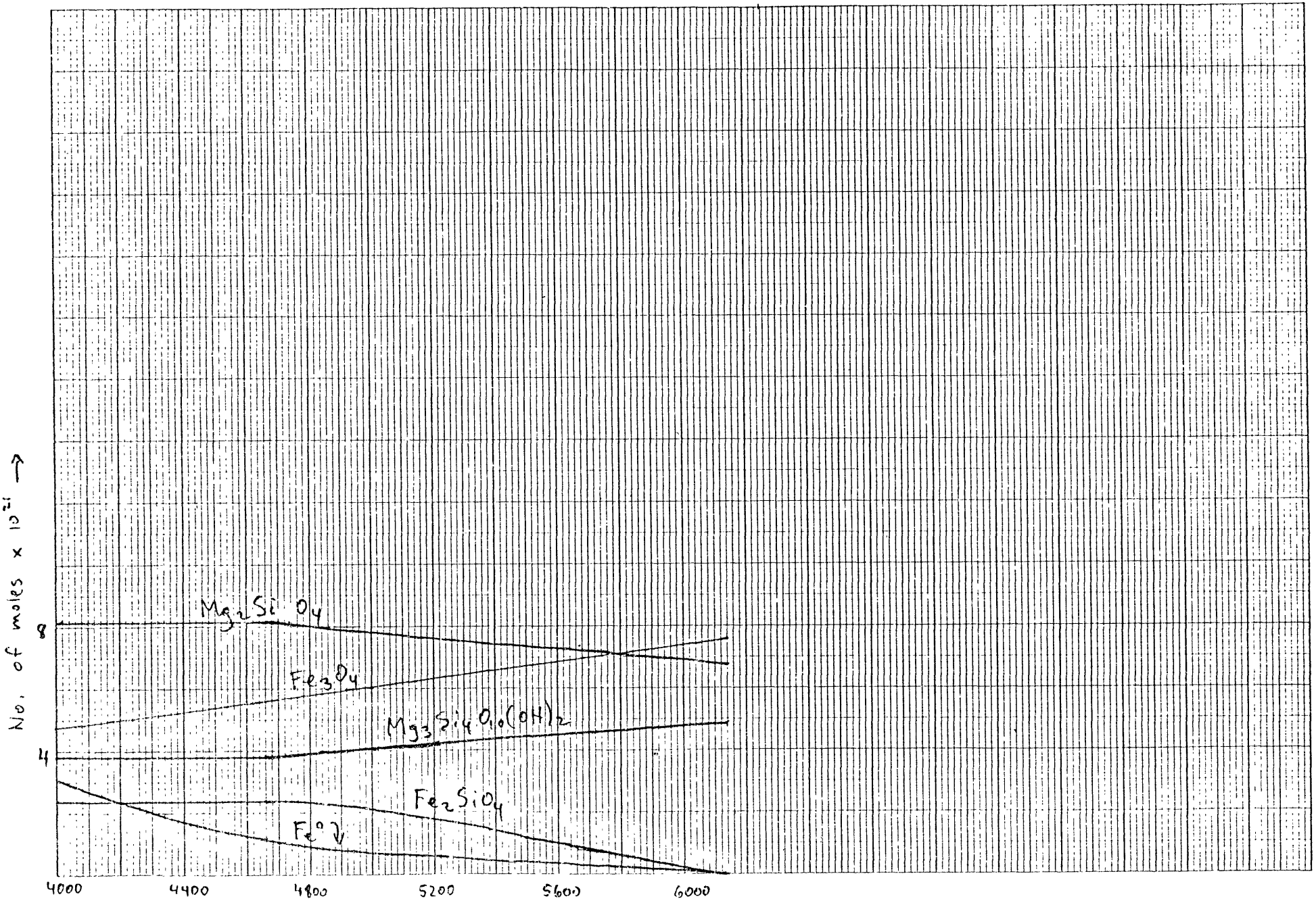

Fig. 17 (cont.)

Caption to Figure 18: The time-dependent evolution during outgassing of the mineralogy of the surface layer of a 95%H + 5%Cl chondrite planet. See caption to Fig. 15.

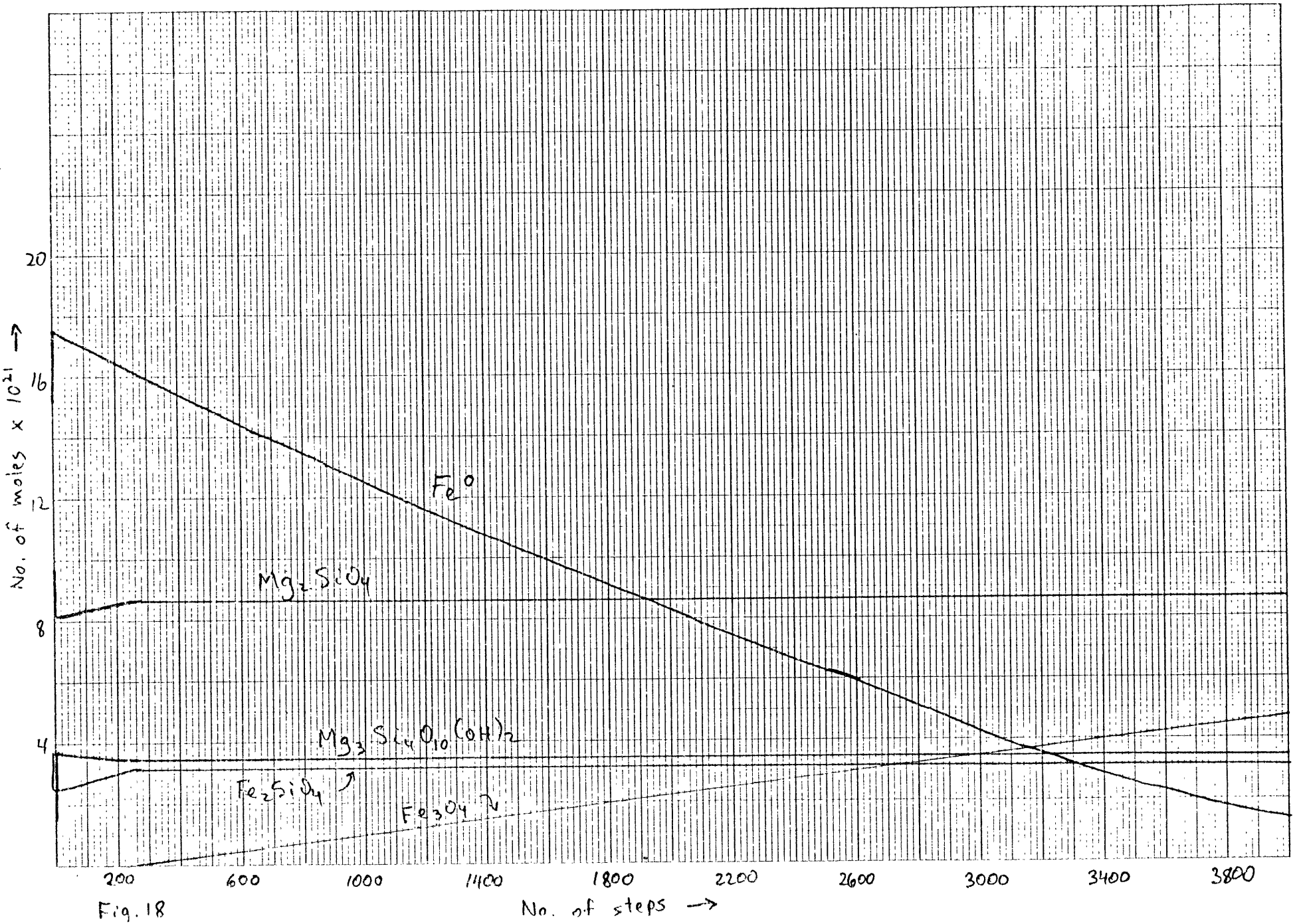

Fig. 18

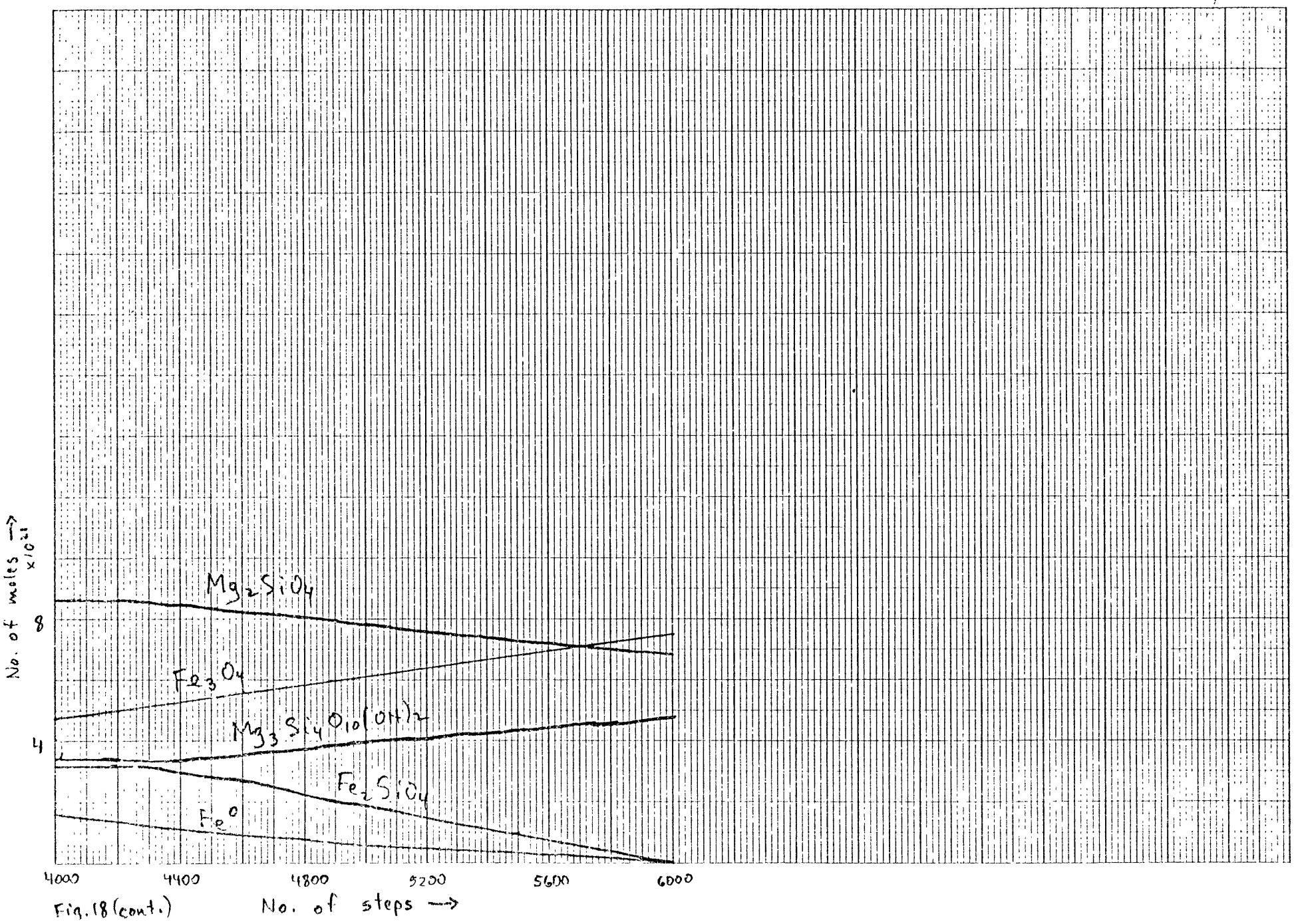

Fig. 18 (cont.)

Caption to Figure 19: The time-dependent evolution during outgassing of the mineralogy of the surface layer of a 90%H + 10%Cl chondrite planet. See caption to Fig. 15.

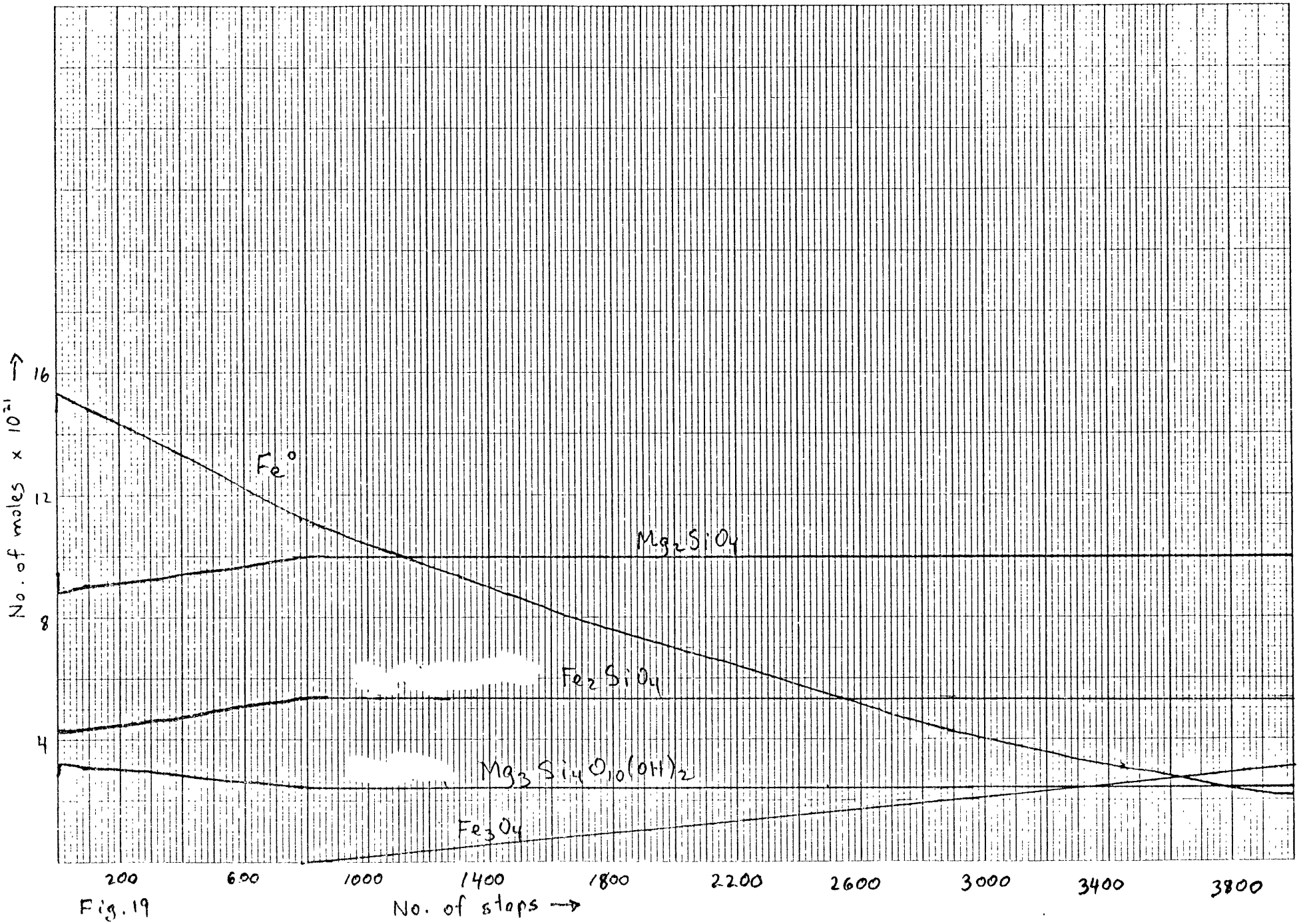

Fig. 19

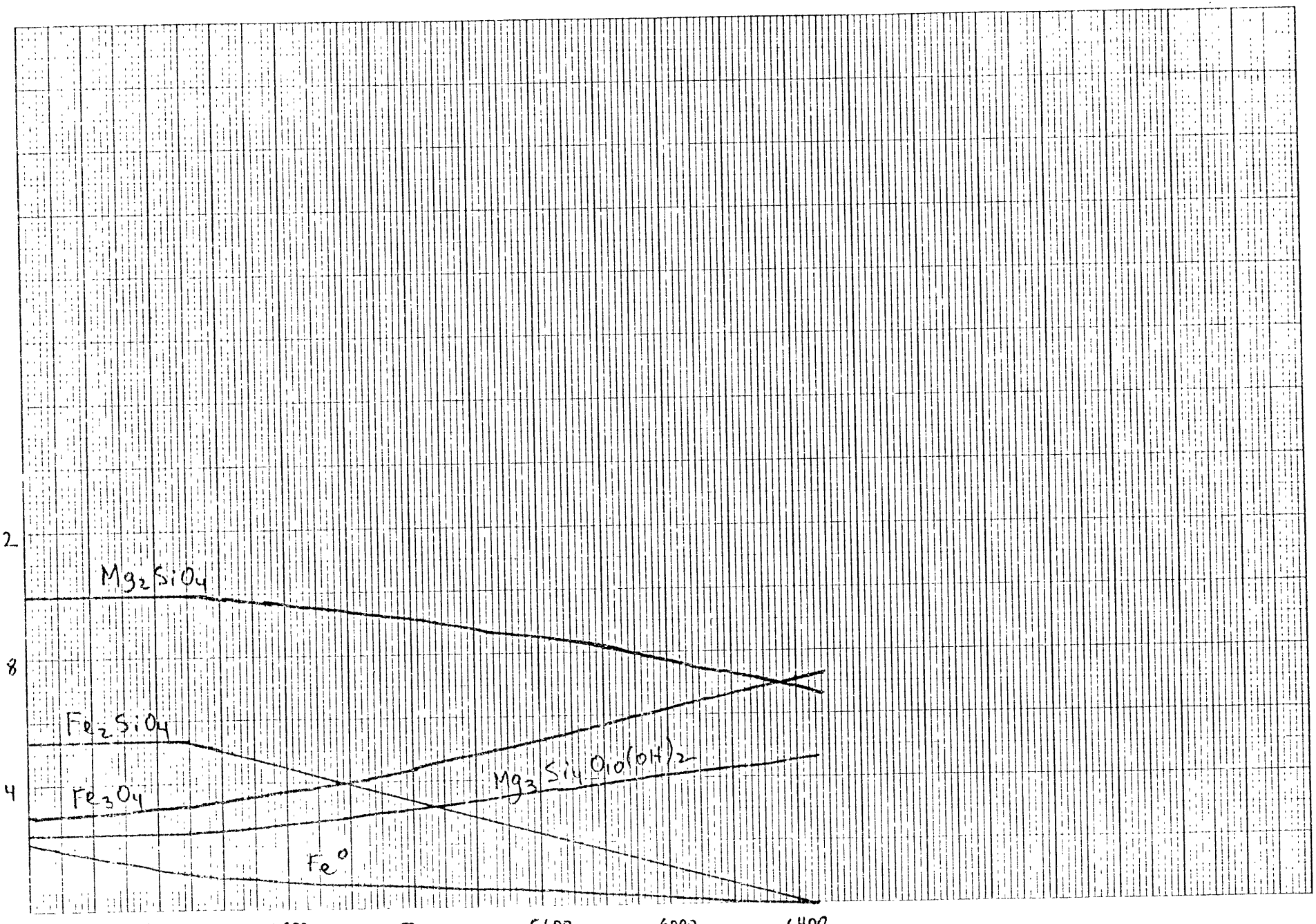

Fig. 17 (cont.)

Acknowledgements

I would like to list everyone who has helped me on this project.

First I must acknowledge my advisor, Dr. John S. Lewis, who first proposed the idea for this thesis and spent many hours of his time inspiring and aiding me. What knowledge I have of cosmochemistry and of the approach to studying the origin and evolution of the Solar System I owe to him.

Next I must thank the students who did their part in formulating this thesis. In particular I must thank Peter Briggs, who together with Guy Consolmagno and Faith Vilas, started this project in the first place. Peter's notes were invaluable to me in helping to set up the computer programs to model the thermal structures of primordial terrestrial planets. Special thanks also go to Steve Barshay and Don Skibo, who helped me with the thermodynamics and computer programming when I first started this project.

Very special thanks are extended to Bruce Fegley, who answered a countless number of my questions, and who bent over backwards to help me in every conceivable way, from loaning me his calculator to providing references to en-

couraging me during the bleak moments of this project.

I would like to thank Cheryl Klink, who provided much needed moral support and kept on encouraging me on to bigger things.

Finally I would like to dedicate this thesis to and especially thank my parents, who provided all the financial and moral support that I needed and more, and who have been eagerly awaiting the completion of this thesis.

References

Ahrens, T. J. (1979) Equations of state of iron sulfide and constraints on the sulfur content of the Earth. J. Geophys. Res. 84, 985-998.

Alexeyeva, K. N. (1958) Physical properties of stony meteorites and their interpretation in the light of hypotheses regarding the origin of the meteorites (in Russian). Meteoritika 16, 68-76.

Anders, E. (1964) Origin, age, and composition of meteorites. Space Sci. Rev. 3, 538-714.

Anders, E. (1968) Chemical processes in the early Solar System, as inferred from meteorites. Acc. Chem. Res. 1, 289-298.

Anders, E. (1971) Meteorites and the early Solar System. Ann. Rev. Astron. Astrophys. 9, 1-34.

Anders, E. and Owen, T. (1977) Mars and Earth: origin and abundance of volatiles. Science 198, 453-465.

Barshay, S. and Lewis, J. S. (1976) Chemistry of primitive solar material. Ann. Rev. Astron. Astrophys. 14, 81-94.

Brace, W. F. and Orange, A. S. (1968) Further studies of the effects of pressure on the electrical resistivity of rocks. J. Geophys. Res. 73, 16, 5407-5420.

Brace, W. F., Silver, E., Hadley, K., Goetze, C. (1972) Cracks and pores: a closer look. Science 178, 162-163.

Cameron, A. G. W. and Pine, M. R. (1973) Numerical models of the primitive solar nebula, Icarus 18, 377-406.

Chapman, C. R. (1976) Asteroids as meteorite parent bodies: the astronomical perspective. Geochim. Cosmochim. Acta 40, 701-719.

Chipman and Elliott (1963) Electric Furnace Steelmaking, vol. II, chap. 16, C. S. Sims, Ed. AIME

Consolmagno, G. (1975) Thermal histories of icy satellites, S.M. thesis, M.I.T.

Cox, L. and Lewis, J. S. (1979) Numerical simulation of the final stages of terrestrial planet accretion. Icarus, in press.

Cox, L., Lewis, J. S., Lecar, M. (1978) A model for close encounters in the planetary problem. Icarus 34, 415-427.

Fanale, F. P. (1971) History of Martian volatiles: implications for organic synthesis. Icarus 15, 279-303.

Gibson, E. K., Moore, C. B., Lewis, C. F. (1971) Total N and C abundances in carbonaceous chondrites. Geochim. Cosmochim. Acta 35, 599-604.

Grossman, L. (1972) Condensation in the primitive solar nebula. Geochim.Cosmochim. Acta 36, 597-619.

Grossman, L. and Larimer, J. W. (1974) Early chemical history of the Solar System. Rev. Geoph. Space Phys. 12, 1, 71-98.

Hall, H. T. and Murthy, V. R. (1974) Magmatic gas additions to the atmosphere and hydrosphere through geologic time. Univ. of Minnesota, preprint.

Hanks, T. C. and Anderson, D. L. (1969) The early thermal history of the Earth. Phys. Earth Planet. Interiors 2, 1, 19-29.

JANAF Thermochemical Tables (1971 and later), compiled by the Thermal Research Lab, Dow Chemical Co., Midland, Michigan.

Larimer, J. S. (1971) Composition of the Earth: chondritic or achondritic? Geochim Cosmochim. Acta 35, 769-786.

Lewis, J. S. (1970) Venus: atmospheric and lithospheric composition. Earth Plan. Sci. Let. 10, 73-80.

Lewis, J. S. (1972a) Low temperature condensation from the solar nebula. Icarus 16, 241-252.

Lewis, J. S. (1972b) Metal/silicate fractionation in the Solar System. Earth Plan. Sci. Let. 15, 286-290.

Lewis, J. S. (1973) Chemistry of the planets. Ann. Rev. Phys. Chem. 24, 339-351.

Lewis, J. S. (1974) The temperature gradient in the solar nebula. Science 186, 440-443.

Lewis, J. S., Barshay, S., Noyes, B. (1979) Primordial retention of carbon by the terrestrial planets. Icarus 37, 190-206.

McCord, T. B. and Gaffey, M. J. (1974) Asteroids surface compositions from reflection spectroscopy. Science 186, 352-355.

Mao, N. (1974) Velocity-density systematics and iron content of the mantle. EOS 55, 416.

Mason, B. (1962) Meteorites, Wiley, New York.

Mason, B. (1963) The carbonaceous chondrites, Space Sci. Rev. 1. 621-646.

Mason, B. (1971) The carbonaceous chondrites: a selective review. Meteoritics 6, 59-79.

Nagy, B. (1975) Carbonaceous meteorites, in Developments in Solar System and Space Science, Vol. 1, Elsevier Scientific Publishing Co.

Ringwood, A. E. (1966) Chemical evolution of the terrestrial planets. Geochim. Cosmochim. Acta 30, 41-42.

Ringwood, A. E. (1966) The chemical composition and origin of the Earth, in Advances in Earth Science, edited by P. M. Hurley, 287-356, M.I.T. Press, Boston.

Ringwood, A. E. (1977) Composition and origin of the Earth, Publication No. 1299, Research School of Earth Sciences, Australian National University, Canberra.

Robie, R. A. and Waldbaum, D. R. (1978) Thermodynamic properties of minerals and related substances at 298.15^{o}K (25.0^{o}C) and one atmosphere (1.013 bars) pressure and at higher temperatures, U.S. Geol. Surv. Bull., No. 1452.

Turekian, K. K. and Clark, S. P. Jr. (1969) Inhomogeneous accumulation of the Earth from the primitive solar nebula. Earth Plan. Sci. Let. 6, 346-348.

Van Schmus, W. R. and Wood, J. A. (1967) A chemical-petrologic classification for the chondritic meteorites. Geochim. Cosmochim. Acta 31, 747-766.

Wasson, J. T. (1974) Meteorites, Springer-Verlag, New York, Heidelberg, Berlin.

Weidenschilling, S. J. (1975) Mass loss from the region of Mars and the asteroid belt. Icarus 26, 361-366.

Wetherill, G. W. (1974) Solar system sources of meteorites and large asteroids. Ann. Rev. Earth Plan. Sci. 2, 303-331.